Stress-induced anisotropic diffusion in alloys: Complex Si solute flow near a dislocation core in Ni

Venkat Manga, Zebo Li, *Thomas Garnier*, *Maylise Nastar*, Pascal Bellon, Robert Averback, **Dallas R. Trinkle**

Materials Science and Engineering, Univ. Illinois, Urbana-Champaign

CEA Saclay, Service de Recherches de Métallurgie Physique, France

Goal: Predict solute and defect evolution near a dislocation

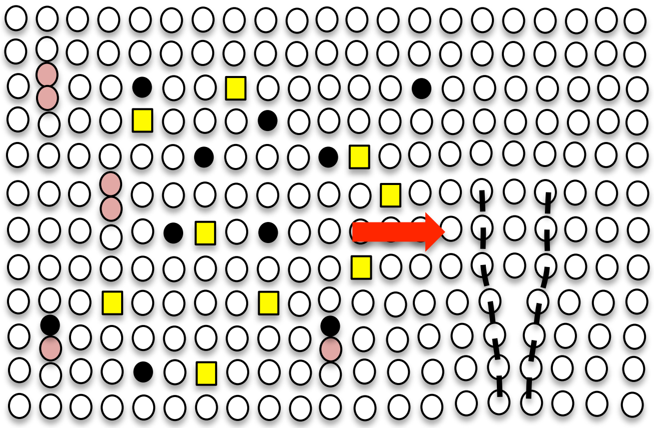

Transport of point defects near dislocations (sinks)

Under irradiation: continuous transport of defect fluxes to sinks

- Coupling of defects and solutes fluxes?
- Segregation, precipitation, creep?

Stresses of dislocation and applied

- Inhomogeneous driving forces
- Inhomogeneous anisotropic mobilities

System: substitutional Si in Ni

Approach:

- Ab initio calculation of migration barriers
- Self-consistent mean-field method

U.S. DEPARTMENT OF ENERGY | Office of Science

BES DE-FG02-05ER46217 & NERSC

Irradiation-induced precipitation

- Undersaturated Ni-Si alloys
  - Precipitation of Ni_3Si precipitates induced by vacancy flux to sinks

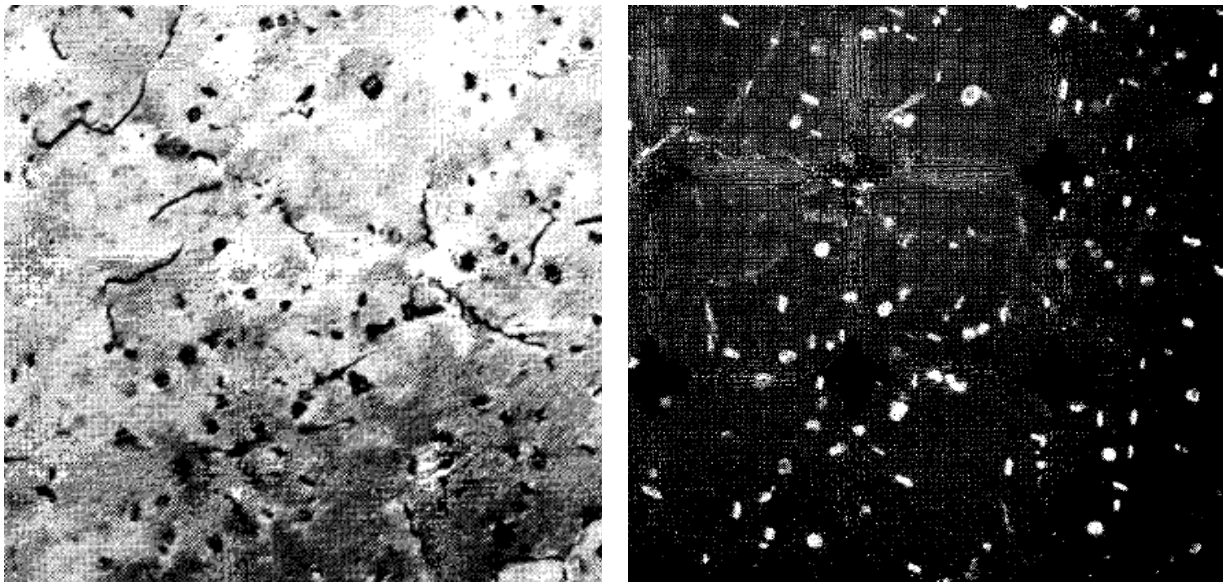

Dislocations

Grain boundaries

Barbu and Ardell, *Scripta metal*.,**9**,(1975)
Rehn *et al., Phys. Rev. B,* **30** (1984)

Composition profiles at dislocation loop in CP304 post-irradiation

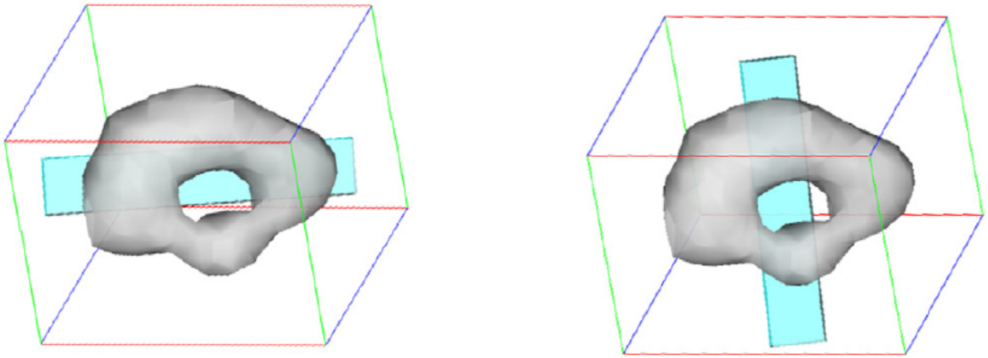

Was *et al.*
Acta Mater. **59**, 1220 (2011)

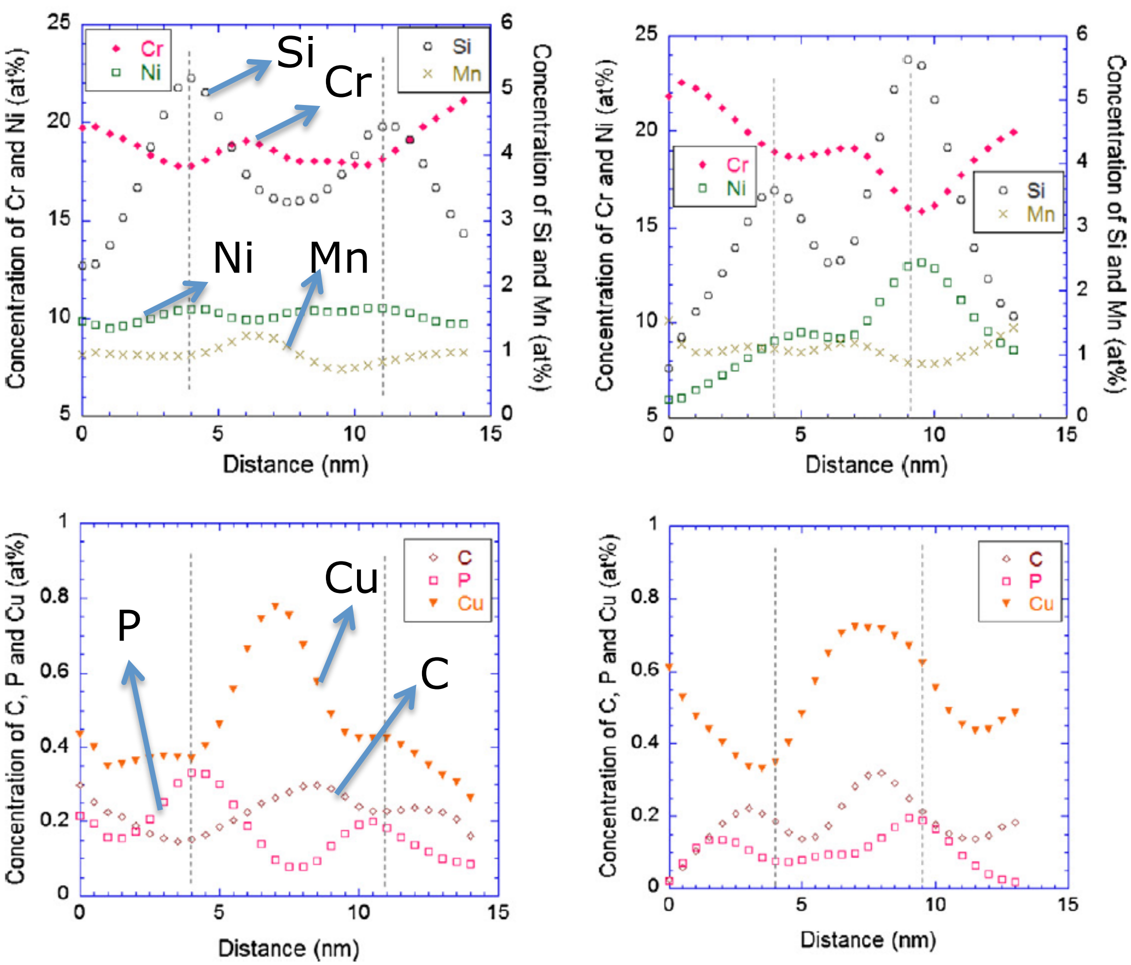

- Enrichment of Si, Ni and P at the dislocation
- Cr and Mn are depleted
- Similar segregation behavior to grain boundaries

Solute drag: vacancy and solute flux coupling

vacancy-solute
exchange dominant

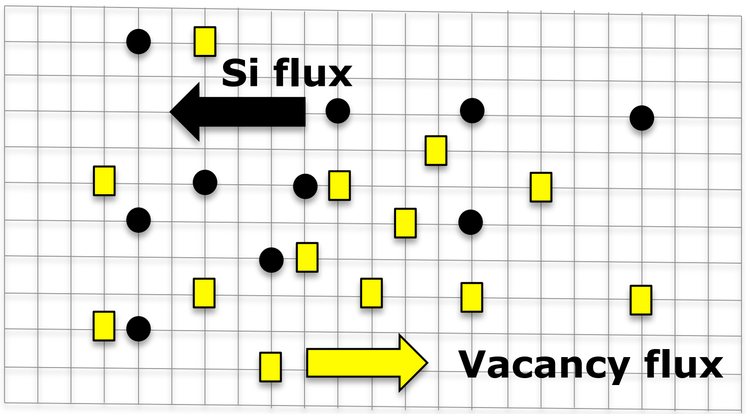

J_V / J_{Si} **negative**
if solutes and vacancies move
in opposite directions

solute drag by
vacancy complex

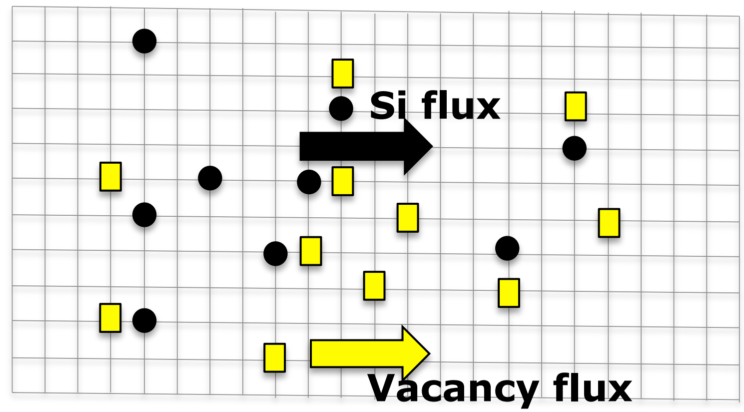

J_V / J_{Si} **positive**
if solutes and vacancies move
in same direction

(a)

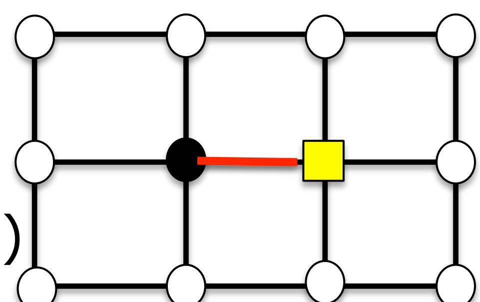

(b)

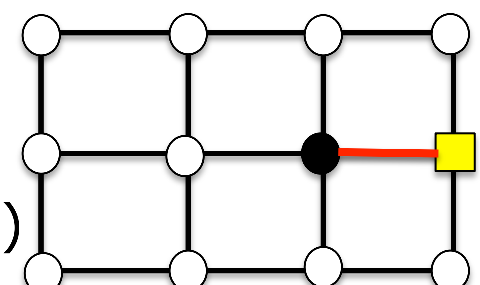

The Onsager flux equations

Linear relation between fluxes and the driving forces (Allnatt1993)

$$J_i = \sum_j L_{ij} X_j \quad \text{(i,j= 1,2,...)}$$

L_{ij} : The phenomenological coefficients;
X : the driving force (for e.g. gradient of chemical potential)

In a binary system Ni-Si

$$J_{\mathrm{Ni}} = L_{\mathrm{NiNi}} \nabla \mu_{\mathrm{Ni}} + L_{\mathrm{NiSi}} \nabla \mu_{\mathrm{Si}} + L_{\mathrm{NiV}} \nabla \mu_{\mathrm{V}}$$
$$J_{\mathrm{Si}} = L_{\mathrm{SiSi}} \nabla \mu_{\mathrm{Si}} + L_{\mathrm{SiNi}} \nabla \mu_{\mathrm{Ni}} + L_{\mathrm{SiV}} \nabla \mu_{\mathrm{V}}$$
$$J_{\mathrm{V}} = L_{\mathrm{VSi}} \nabla \mu_{\mathrm{Si}} + L_{\mathrm{VNi}} \nabla \mu_{\mathrm{Ni}} + L_{\mathrm{VV}} \nabla \mu_{\mathrm{V}}$$

$$\sum_i J_i = 0$$

vacancy-mediated diffusion

Quantities of interest from phenomenological coefficients

Diffusion coefficients

$$D_{\mathrm{Si}} = \frac{kT}{n}\left(\frac{L_{\mathrm{SiSi}}}{c_{\mathrm{Si}}} - \frac{L_{\mathrm{NiSi}}}{c_{\mathrm{Ni}}}\right)\left(1 + \frac{\partial \ln \gamma_{\mathrm{Si}}}{\partial \ln c_{\mathrm{Si}}}\right)$$

In the dilute limit (c_{Si}<<1)

$$D_{\mathrm{Si}} = \frac{kT}{n_{\mathrm{Si}}} L_{\mathrm{SiSi}}$$

γ_{si} -- activity coefficient
c_{si} -- concentration of Si

Solute drag

$$L_{\mathrm{SiV}} = -L_{\mathrm{SiSi}} - L_{\mathrm{NiSi}} \qquad G = \frac{L_{NiSi}}{L_{SiSi}}$$

L_{SiV} - negative if solutes and vacancies move in opposite directions
- positive if **solute-drag** is predominant

Allnatt: *Atomic transport in solids* (1993)

Vacancy mediated diffusion in FCC Ni

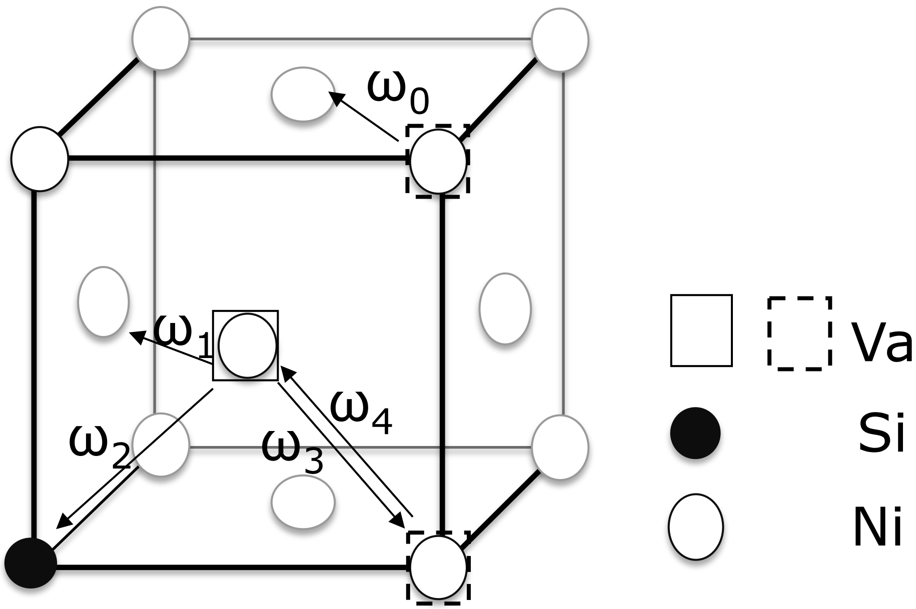

	Jump type
ω_0	self-diffusion jump
ω_1	vacancy-exchange
ω_2	impurity jump
ω_3	dissociation jump
ω_4	association jump

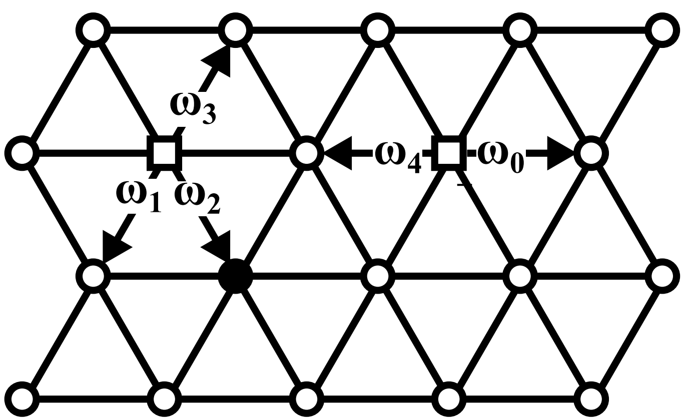

(111) plane

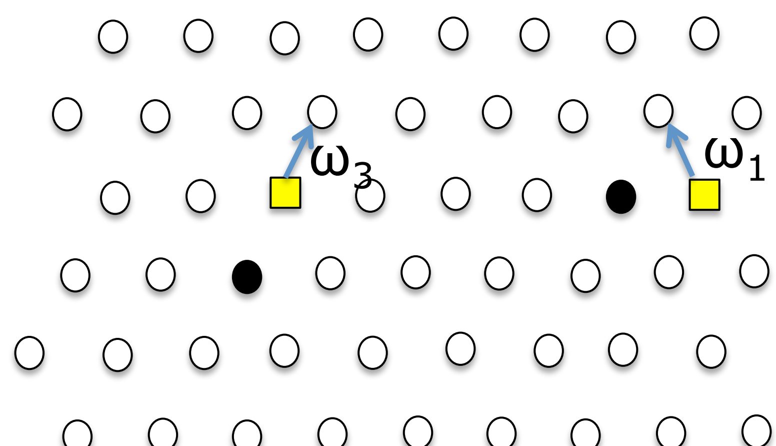

$\omega_3 << \omega_1$: Si-Va tightly bound = Si in the same direction as vacancies

$\omega_3 \approx \omega_1$: Si-Va no strong interaction = Si flows opposite to vacancies

Jump frequencies: harmonic transition state theory

atomic jump freq.

$$\omega = \frac{\prod_{3N} \nu_i^{IS}}{\prod_{3N-1} \nu_i^{TS}} \exp\left(-\frac{\Delta F_{ele}^{TS-IS}}{k_B T}\right) \exp\left(-\frac{\Delta H_{mig}^{TS-IS}}{k_B T}\right)$$

phonon frequency

enthalpy of migration

First-Principles calculation of

- Phonon frequencies 'v' within harmonic approximation
- Thermal electronic contribution from electronic density of states
- Enthalpy of migration from nudged-elastic band method

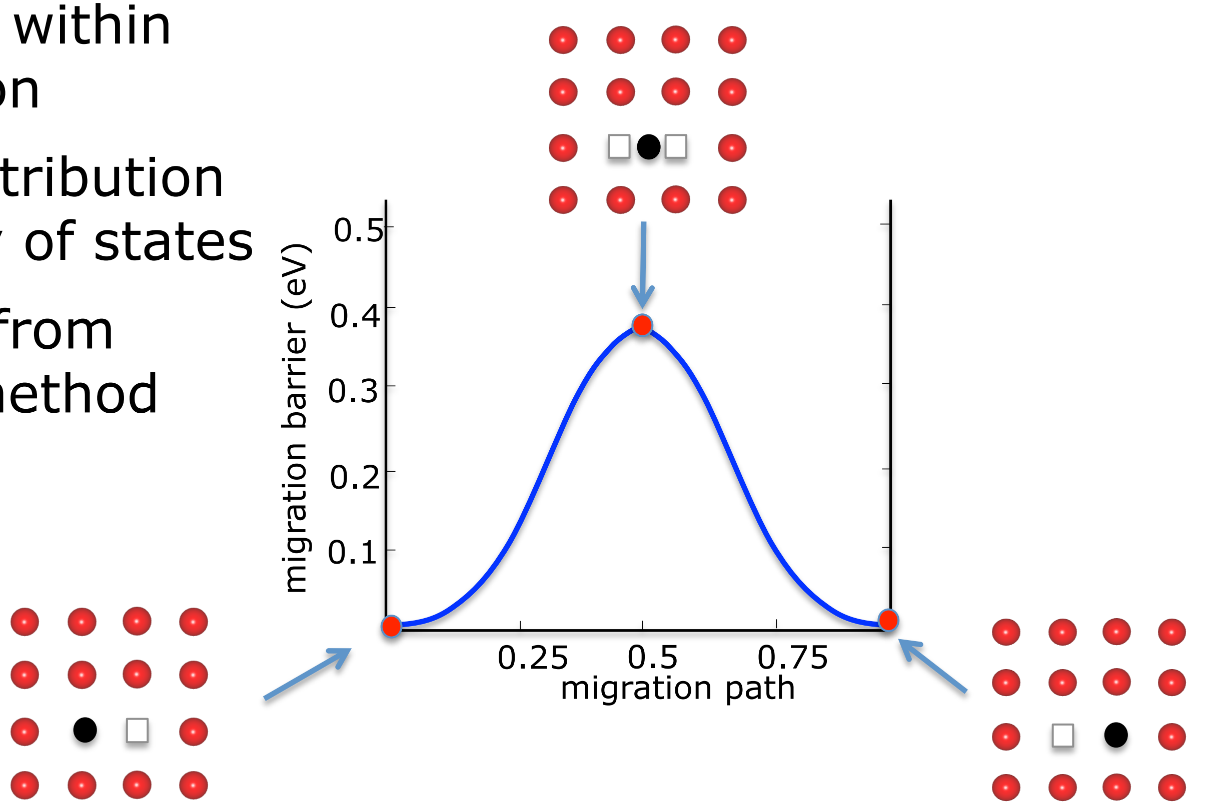

Phenomenological coefficients modified by strains

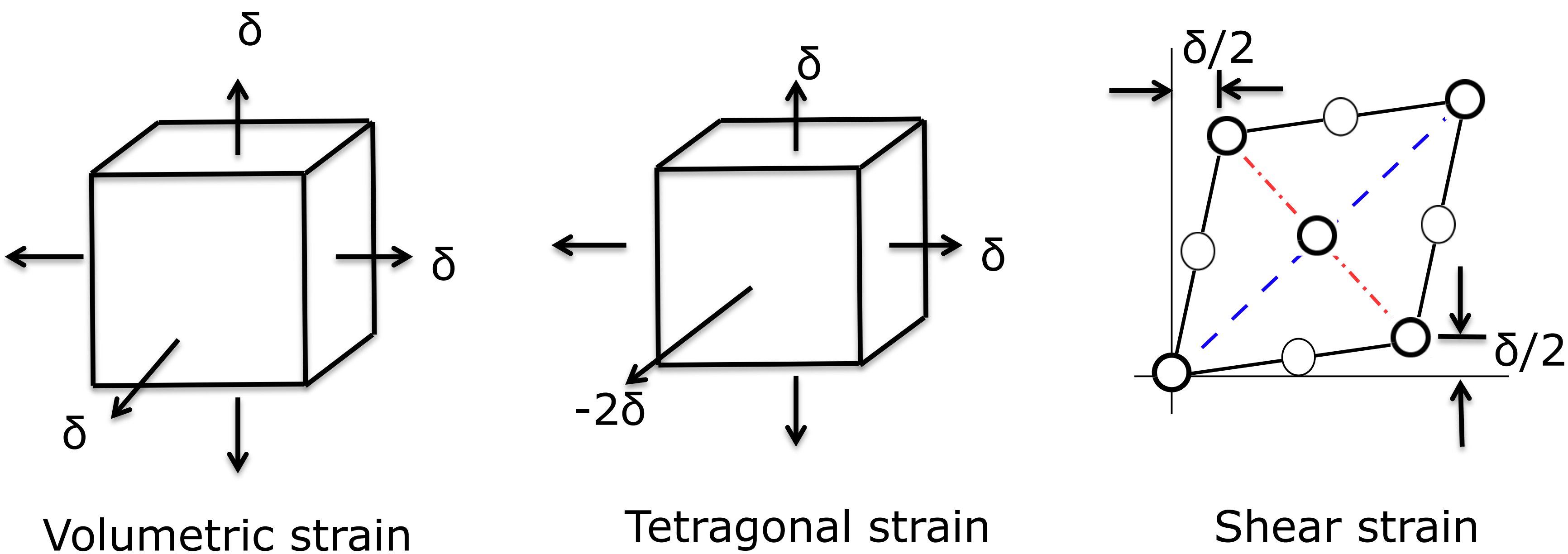

L_{ij} (δ) : phenomenological coefficients as a function of strain

$$\omega_j(\delta) = \nu^*(\delta)\cdot\exp\left(\frac{-\Delta E_j(\delta)}{kT}\right)$$ From ab initio calculations

$$L_{\mathrm{SiV}}(\omega_0,\omega_1,\omega_2\ldots)$$ From self-consistent mean-field[1,2]

$$L_{\mathrm{SiV}}(\delta) = L_{\mathrm{SiV}}(0) + \left.\frac{dL_{\mathrm{SiV}}}{d\delta}\right|_{\delta=0}\cdot\delta$$

1. Nastar et al. Phil. Mag. (2005), 2. Nastar et al. Phil. Mag. A (2000)

Vacancy-mediated diffusion with hydrostatic strain

- The planar cage for any <110> jump
- Strain on the cage area and its relation to the barriers

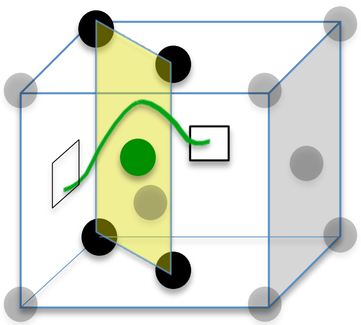

<110> jumps

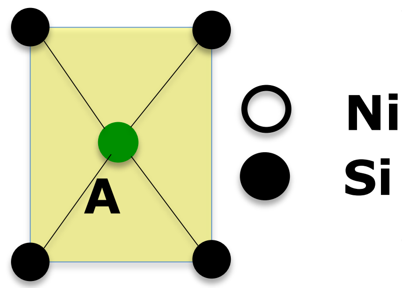

cage at the transition state

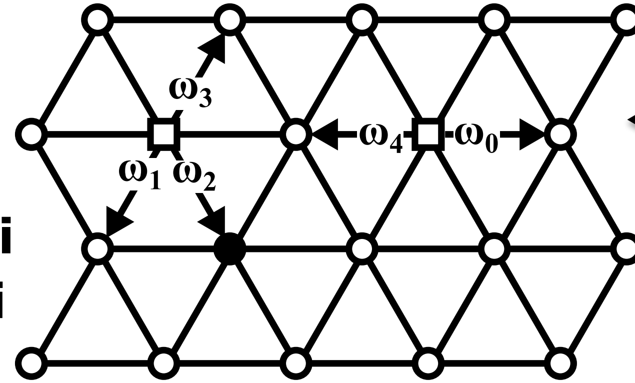

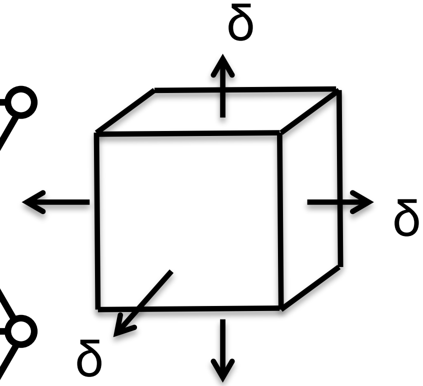

- 5-frequency model for FCC
- No change in the symmetry under volumetric strain

Strain on the cage diagonal : δ

	Jump type		**Tension** (δ=0.01)	δ=0	**Compression** (δ=-0.01)
ω_0	self-diffusion jump	Barriers [eV]	1.04 ≈ 1.10–0.07	1.10	1.17 = 1.10+0.07
ω_1	vacancy-exchange		0.99 ≈ 1.05–0.07	1.05	1.12 = 1.05+0.07
ω_2	impurity jump		0.87 = 0.94–0.07	0.94	1.01 = 0.94+0.07
ω_3	dissociation jump		1.20 = 1.27–0.07	1.27	1.34 = 1.27+0.07
ω_4	association jump		1.10 ≈ 1.16–0.07	1.16	1.23 = 1.16+0.07

All barriers change by the same quantity with strain: $\Delta E_i(\delta) \approx \Delta E_i(0) - (7\text{eV})\delta$

Diffusion coefficient of Si in Ni: hydrostatic strain

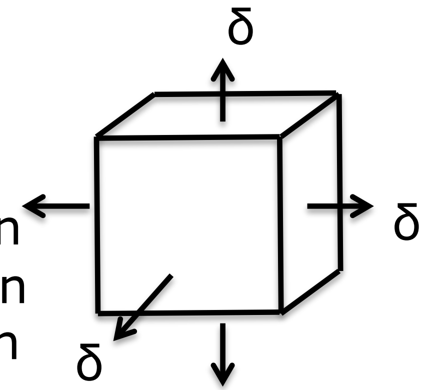

- Calculations similar to the 5-frequency model
  - 14 frequencies when including 3rd neighbor interaction
  - 1st neigh. 0.1eV attraction, 3rd neigh. 0.05eV repulsion
  - Most hop barriers follow kinetically-resolved activation barrier approx.: forward-reverse average ≈ constant
- Same change in activation energies with stress for all jumps

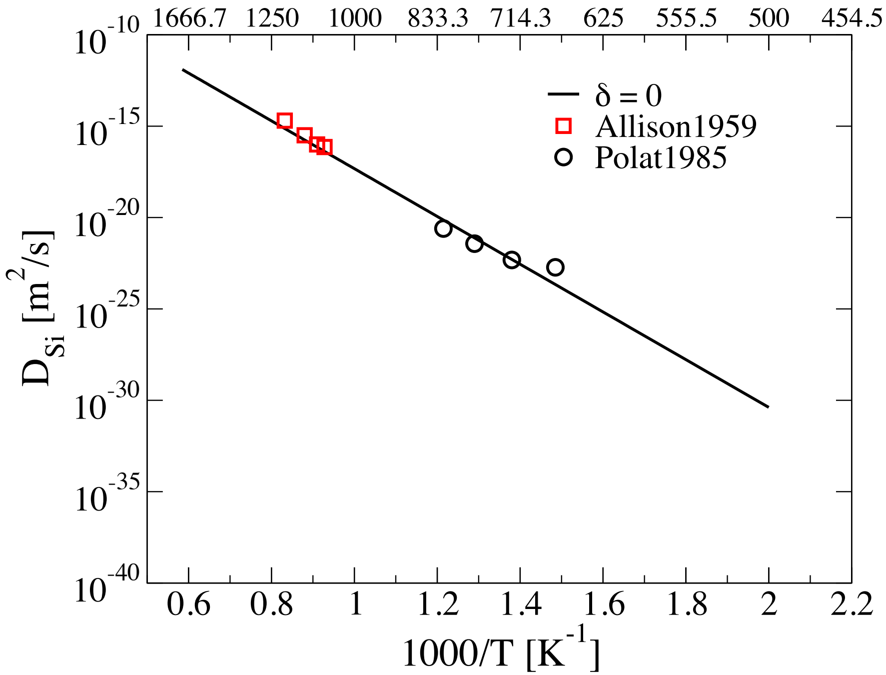

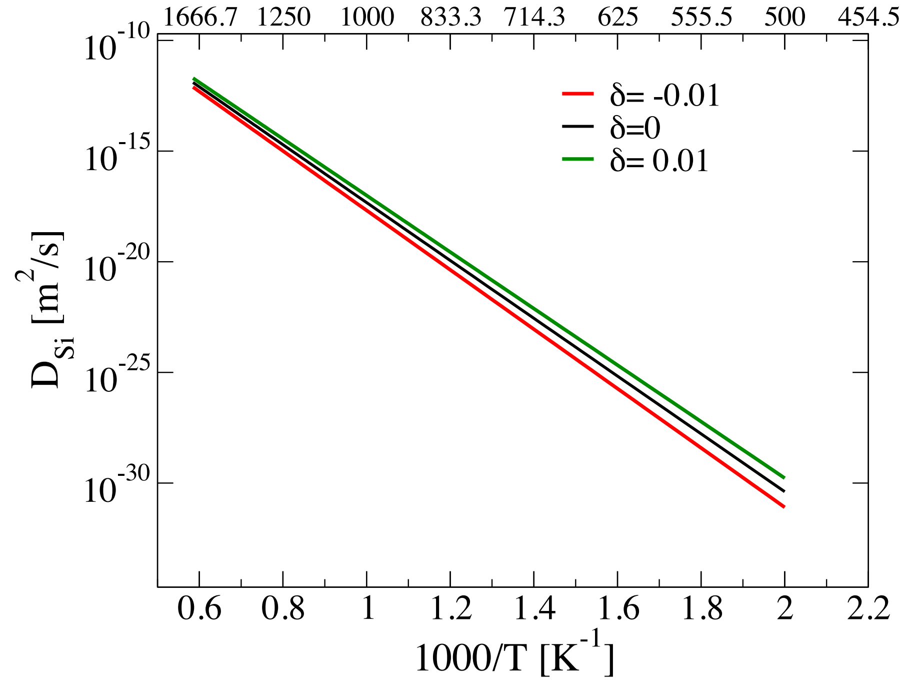

Calculated diffusivities match the experimental data

Mobility coefficients of Si in Ni: solute drag

- From the 14 frequency model

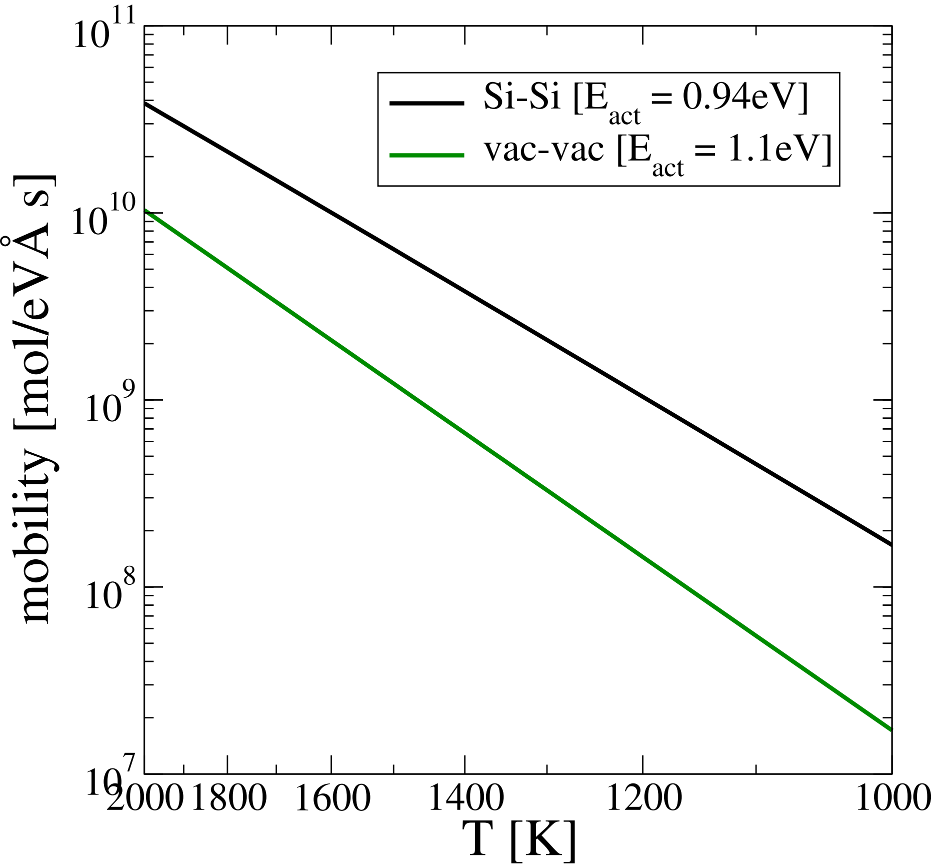

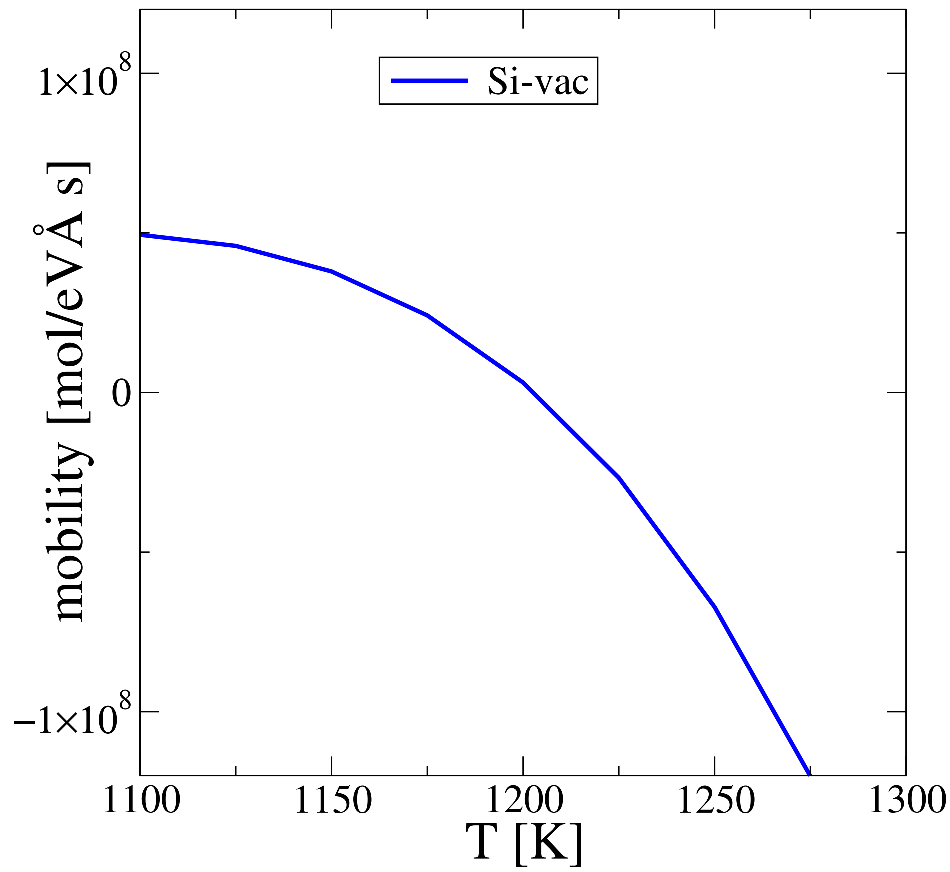

Small change in vacancy wind with **volumetric** strain

Mobility coefficients of Si in Ni: vacancy wind

- From the 5 frequency model: crossover temperature of 1200K

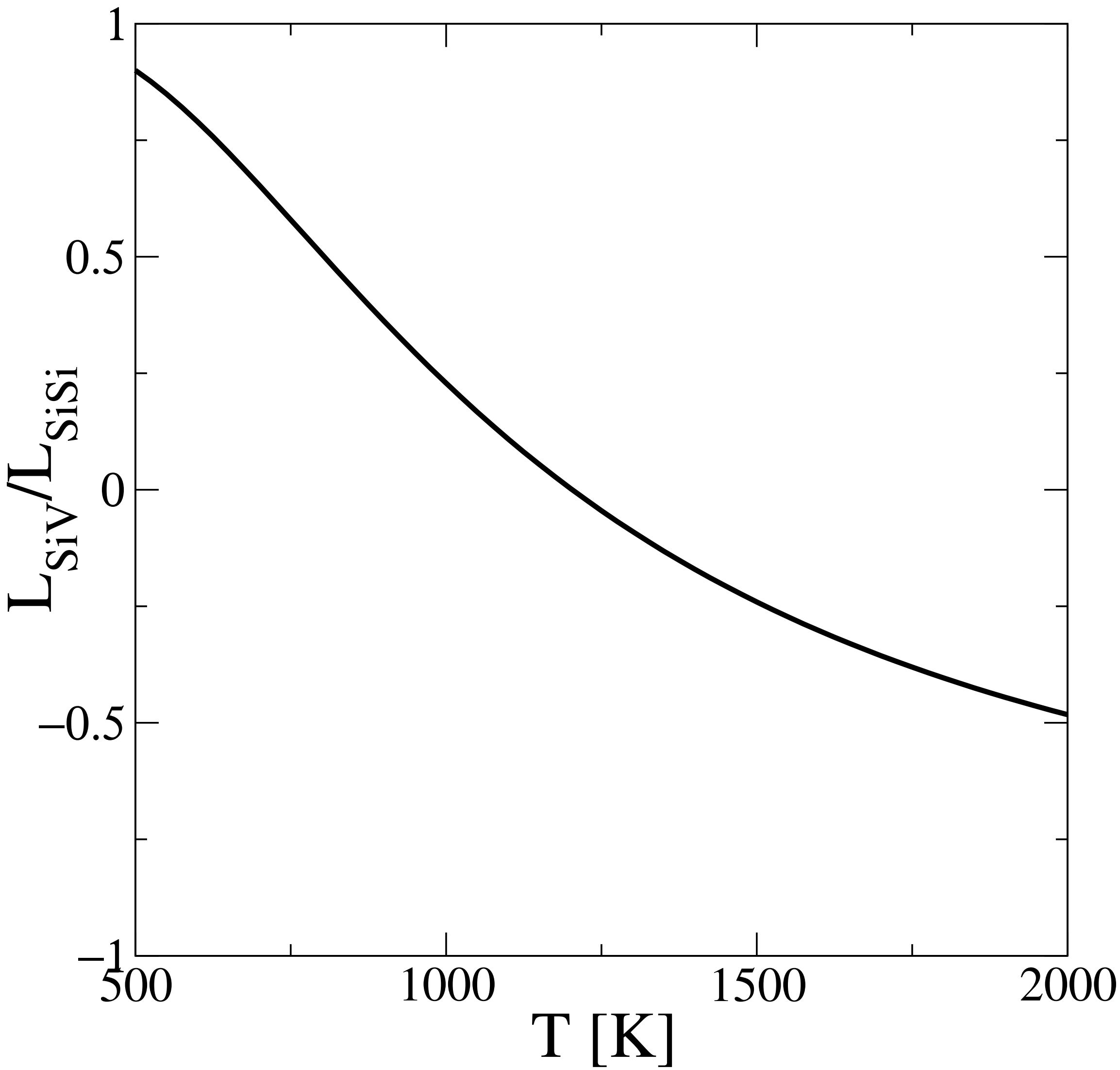

$$\frac{1}{L_{\mathrm{SiV}}}\frac{\partial L_{\mathrm{SiV}}}{\partial \varepsilon_{\mathrm{volume}}} \approx 68$$

for T=1100-1300K

Small change in vacancy wind with **volumetric** strain

Migration barriers and jump frequencies: tetragonal strain

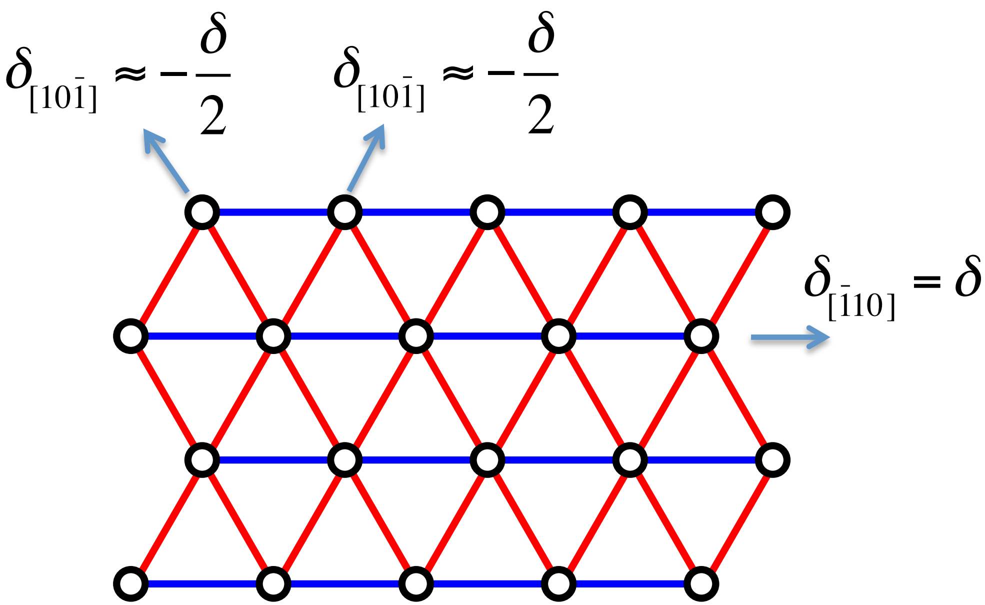

(111) Plane : Tetragonal strain

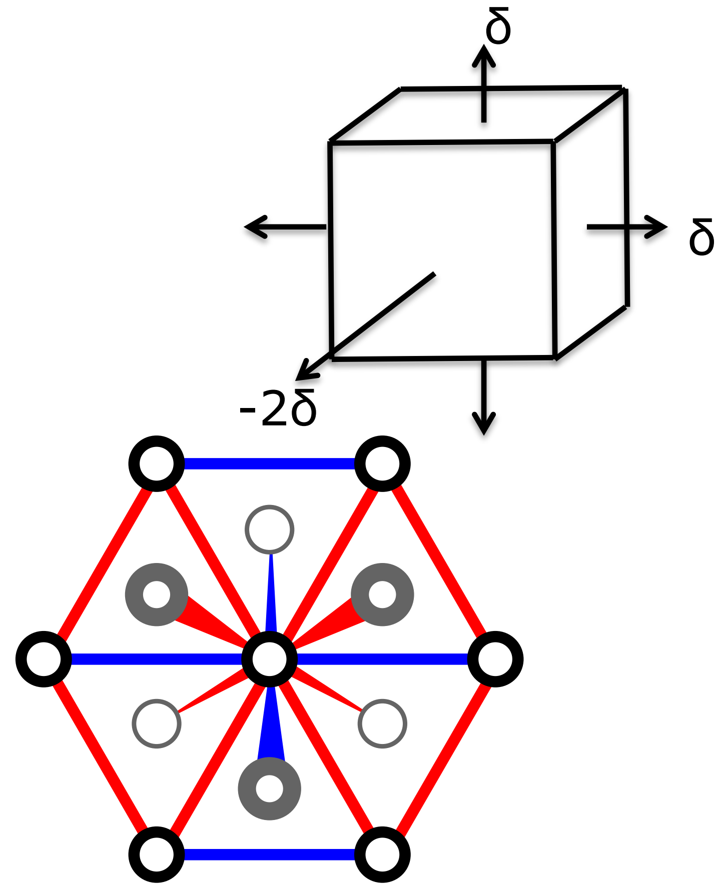

12 first nearest neighbor(NN) bonds break symmetry <110>:
Red (8) and Blue (4)

δ>0 – Blue bonds are longer than Red
δ<0 – Blue bonds are shorter than Red

$\boldsymbol{\delta_b = \delta}$
$\boldsymbol{\delta_r = -\delta/2}$

Needs 15 (44) frequencies to calculate L_{ij} matrix

Ni self-diffusion jumps (ω_0 –type) under tetragonal strain

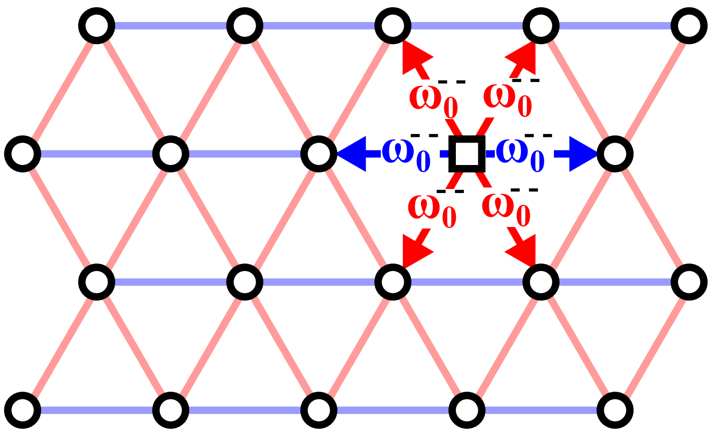

δ_b = δ and δ_r = -δ/2;
with δ= ± 0.01

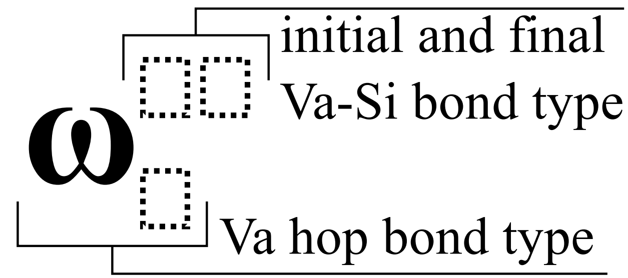

ω_0	ω_0^{--}, ω_0^{--}

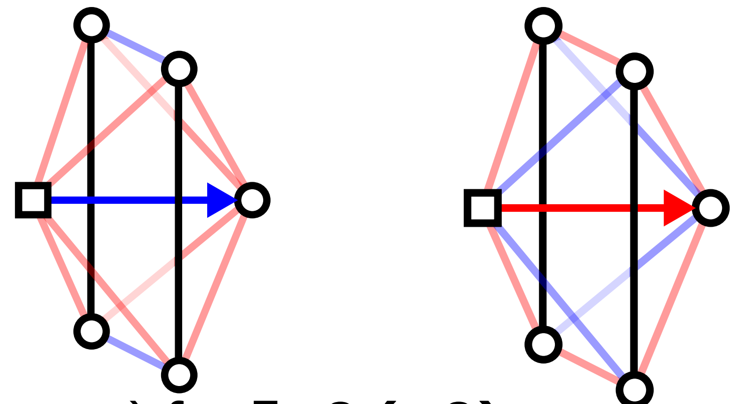

The degeneracy is lost due to strain:
12 ΔE_0 split into : 8 ΔE_0^{--} and 4 ΔE_0^{--}

For a strain δ = 0.01 diagonal of the cage
Contracts (by -0.01) – for Blue jump
Expands (by 0.005) – for Red jump

- Blue Jumps (ΔE_0) increase (decrease) for **δ>0 (<0)**
- Red Jumps (ΔE_0) decrease (increase) for **δ >0 (<0)**

	Strain: +0.01		Strain: 0		Strain: -0.01	
Barrier (eV)	ΔE_0^{--}	1.24 ≈1.10+0.14	ΔE_0	1.10	ΔE_0^{--}	0.96 ≈ 1.10-0.14
	ΔE_0^{--}	1.02 ≈1.10-0.07			ΔE_0^{--}	1.16 ≈ 1.10+0.07

$$\Delta E_0(\delta) \approx \Delta E_0(0) - (14\text{eV})\delta_{\text{diagonal}}$$

Si-vacancy exchange (ω_2 –type) under tetragonal strain

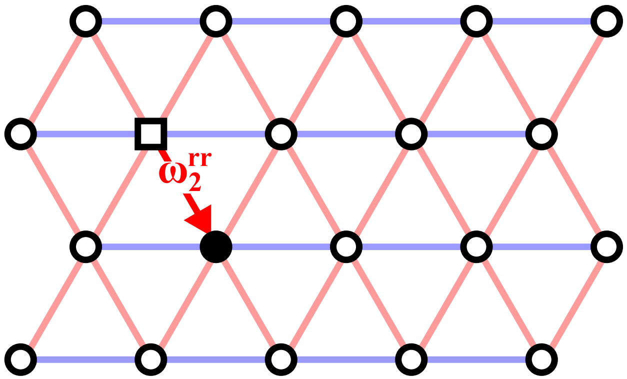

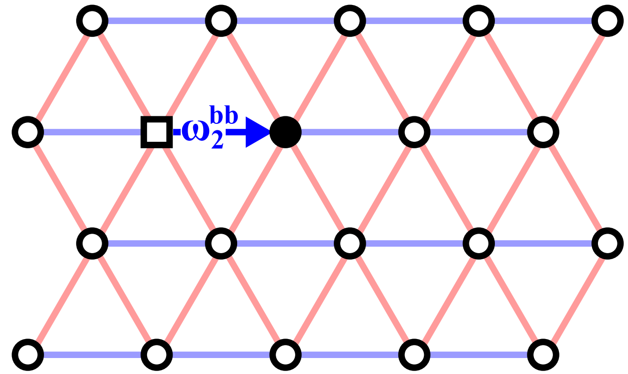

δ_b = δ and δ_r = -δ/2;
with δ= ± 0.01

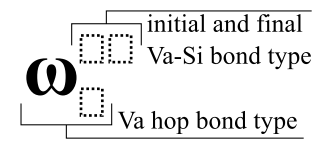

ω_2	ω_2^{rr}, ω_2^{bb}

The degeneracy is lost due to strain:
12 ΔE_0 split into : 8 ΔE_2^{rr} and 4 ΔE_0^{bb}

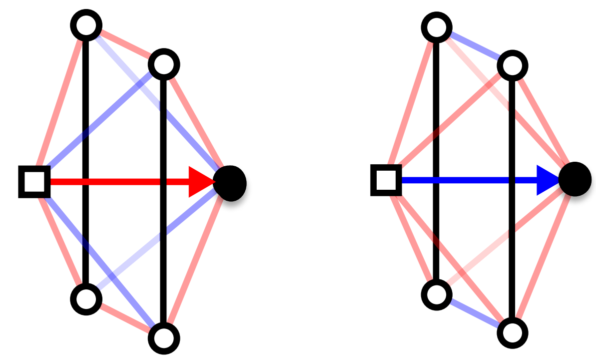

For a strain δ = 0.01 diagonal of the cage
Contracts (by -0.01) – for Blue jump
Expands (by 0.005) – for Red jump

- Blue Jumps (ΔE_2) increase (decrease) for **δ>0 (<0)**
- Red Jumps (ΔE_2) decrease (increase) for **δ >0 (<0)**

	Strain: +0.01		Strain: 0		Strain: -0.01	
Barrier (eV)	ΔE_2^{bb}	1.07 ≈ 0.94+0.14	ΔE_2	0.94	ΔE_2^{bb}	0.80 ≈ 0.94-0.14
	ΔE_2^{rr}	0.86 ≈ 0.94-0.07			ΔE_2^{rr}	1.00 ≈ 0.94+0.07

$$\Delta E_2(\delta) \approx \Delta E_2(0) - (14\text{eV})\delta_{\text{diagonal}}$$

Si-Va swing (ω_1 –type) under tetragonal strain

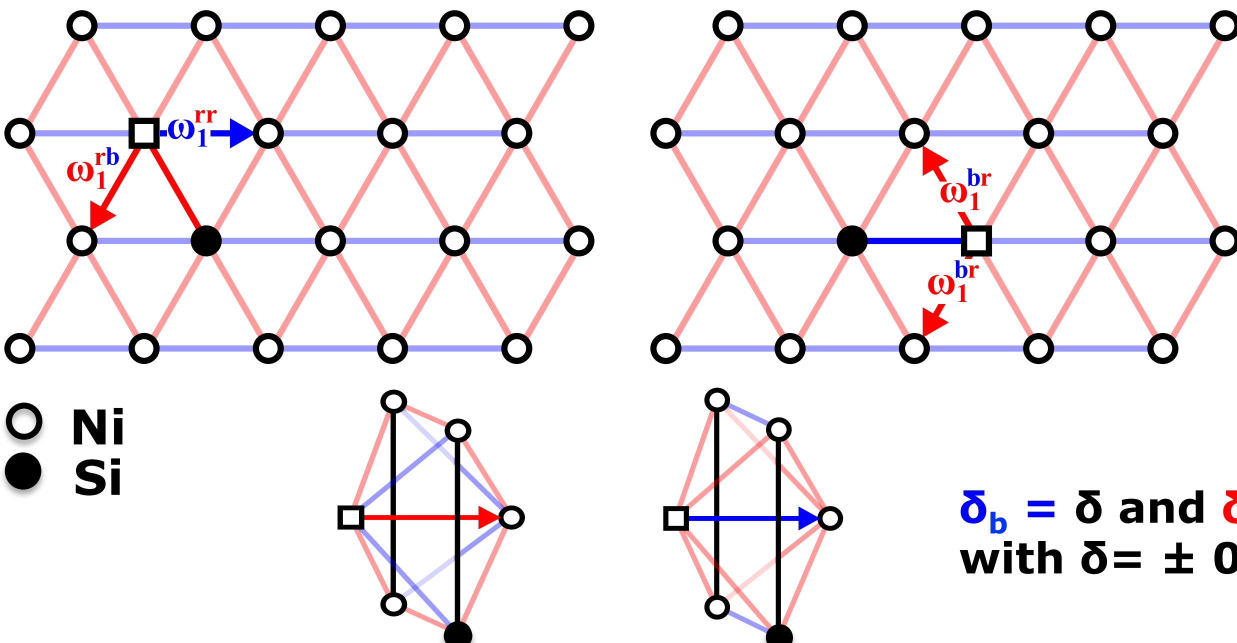

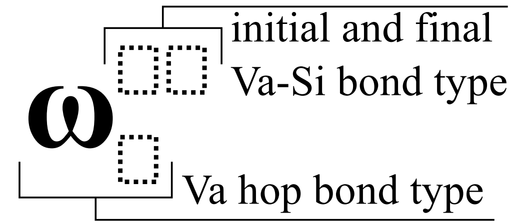

ω_1	ω_1^{rb}, ω_1^{rr}, ω_1^{br}

δ_b = δ and δ_r = -δ/2;
with δ= ± 0.01

- Blue Jumps (ΔE_2) increase (decrease) for **δ>0 (<0)**
- Red Jumps (ΔE_2) decrease (increase) for **δ >0 (<0)**

	Strain: +0.01		Strain: 0		Strain: -0.01	
Barrier (eV)	ΔE_1^{rr}	1.18 ≈ 1.05+0.14	ΔE_1	1.05	ΔE_1^{rr}	0.92 ≈ 1.05-0.14
	ΔE_1^{rb}	0.98 ≈ 1.05-0.07			ΔE_1^{rb}	1.11 ≈ 1.05+0.07
	ΔE_1^{br}	0.98 ≈ 1.05-0.07			ΔE_1^{br}	1.11 ≈ 1.05+0.07

Si-Va re-orientation can happen faster along particular directions

$$\Delta E_1(\delta) \approx \Delta E_1(0) - (14\text{eV})\delta_{\text{diagonal}}$$

Si-Va dissociation jump (ω_3 –type) under tetragonal strain

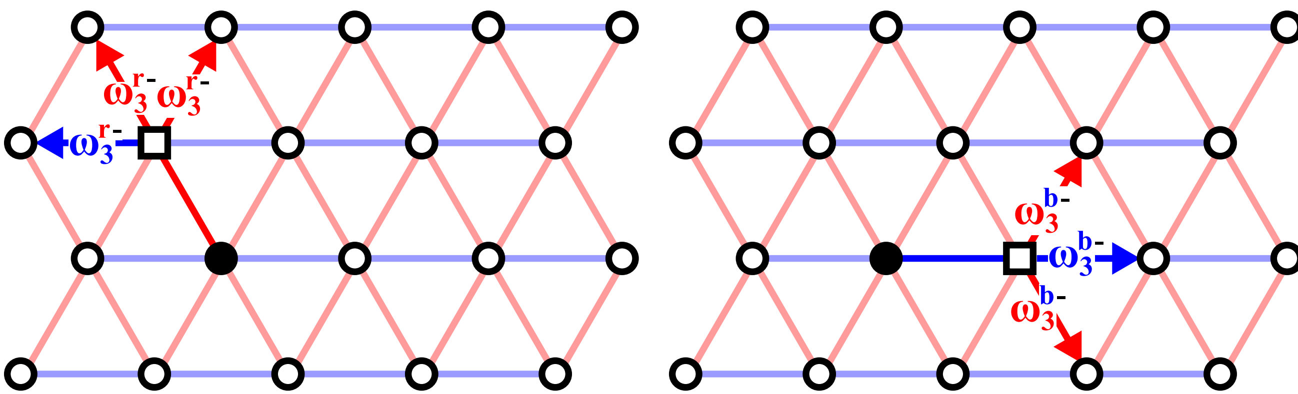

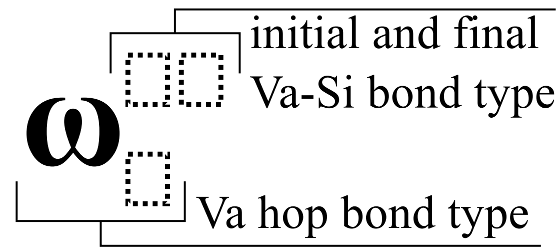

ω_3	ω_3^{r-}, ω_3^{b-}, ω_3^{b-}, ω_3^{r-}

δ_b = δ and δ_r = -δ/2

- Blue Jumps (ΔE_3) increase (decrease) for **δ>0 (<0)**
- Red Jumps (ΔE_3) decrease (increase) for **δ >0 (<0)**

	Strain: +0.01		Strain: 0		Strain: -0.01	
Barrier (eV)	ΔE_3^{b-}	1.41 ≈ 1.27+0.14	ΔE_3	1.27	ΔE_3^{b-}	1.12 ≈ 1.27−0.14
	ΔE_3^{r-}	1.40 ≈ 1.27+0.14			ΔE_3^{r-}	1.11 ≈ 1.27−0.14
	ΔE_3^{r-}	1.18 ≈ 1.27−0.07			ΔE_3^{r-}	1.34 ≈ 1.27+0.07
	ΔE_3^{b-}	1.18 ≈ 1.27−0.07			ΔE_3^{b-}	1.34 ≈ 1.27 - 0.07

$$\Delta E_3(\delta) \approx \Delta E_3(0) - (14\text{eV})\delta_{\text{diagonal}}$$

Si-Va association jump (ω_4 –type) under tetragonal strain

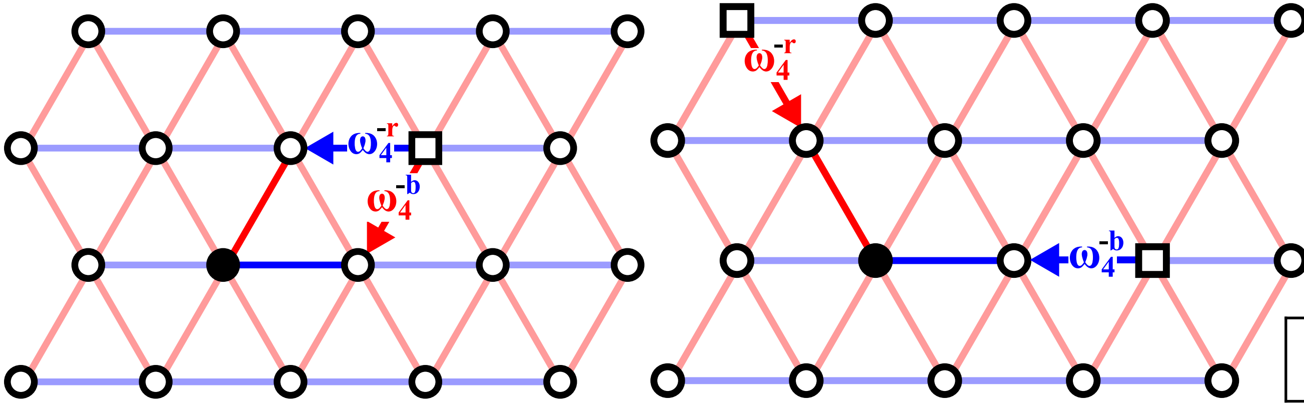

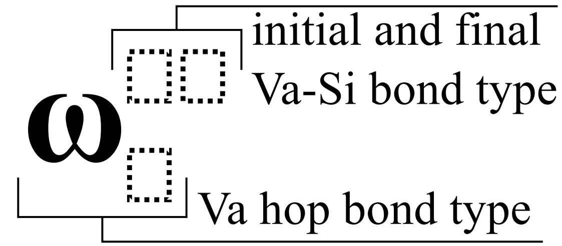

ω_4	ω_4^{-r}, ω_4^{-b}, ω_4^{-b}, ω_4^{-r}

$\delta_b = \delta$ and $\delta_r = -\delta/2$

- Blue Jumps (ΔE_4) increase (decrease) for **δ>0 (<0)**
- Red Jumps (ΔE_4) decrease (increase) for **δ >0 (<0)**

	Strain: +0.01		Strain: 0		Strain: -0.01	
Barrier (eV)	ΔE_4^{-b}	1.29 ≈ 1.16+0.14	ΔE_4	1.16	ΔE_4^{-b}	1.02 ≈ 1.16-0.14
	ΔE_4^{-r}	1.29 ≈ 1.16+0.14			ΔE_4^{-r}	1.00 ≈ 1.16-0.14
	ΔE_4^{-r}	1.09 ≈ 1.16-0.07			ΔE_4^{-r}	1.21 ≈ 1.16+0.07
	ΔE_4^{-b}	1.08 ≈ 1.16-0.07			ΔE_4^{-b}	1.22 ≈ 1.16+0.07

$$\Delta E_4(\delta) \approx \Delta E_4(0) - (14\text{eV})\delta_{\text{diagonal}}$$

Summary: All jump barriers under tetragonal strain

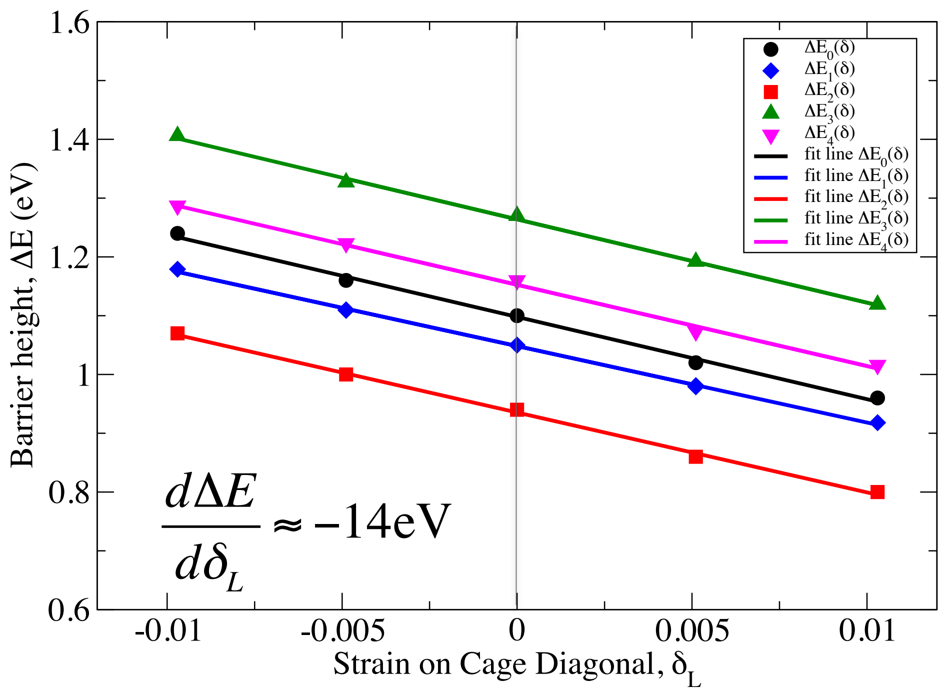

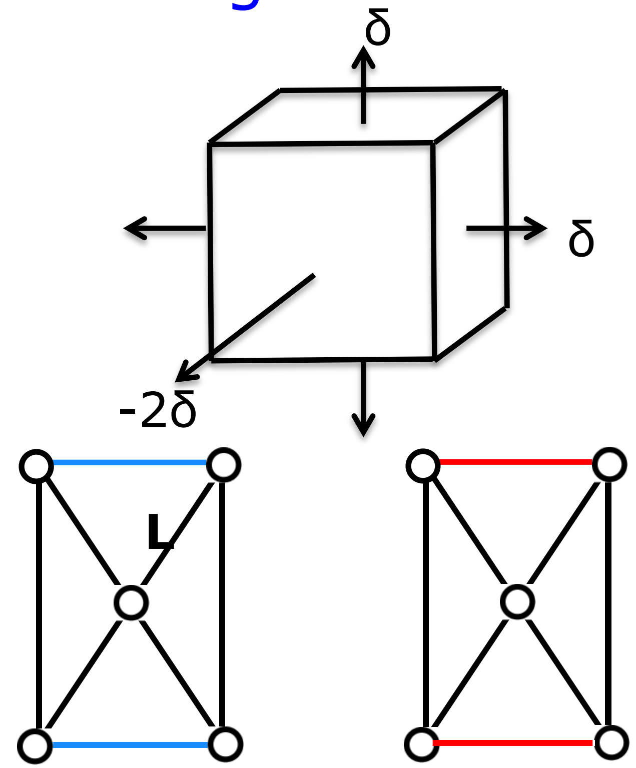

Blue jump   Red jump

A constant $\frac{d\Delta E}{d\delta_L}$ is found on all jump types $\Delta E_j(\delta_L) \approx \Delta E_j(0) - 14\text{eV}\ \delta_L$

Changes in the cage-diagonal explains the changes in the migration barriers

The blue jumps: $\Delta E_i(\delta) \approx \Delta E_i(0) + 14\text{eV}\ \delta$

The red jumps: $\Delta E_i(\delta) \approx \Delta E_i(0) - 7\text{eV}\ \delta$

Symmetry enforces −2:1 ratio for derivative

Kinetic Coupling: Self-Consistent Mean-Field Model

Vaks (1993);
Nastar *et al.* (2000; 2005; 2007)
Garnier and Nastar (2011)

- Microscopic Master equation

$$\frac{d\hat{P}(\mathbf{n},t)}{dt} = \sum_{\tilde{\mathbf{n}}} \hat{W}(\tilde{\mathbf{n}} \to \mathbf{n})\hat{P}(\tilde{\mathbf{n}},t) - \sum_{\mathbf{n}} \hat{W}(\mathbf{n} \to \tilde{\mathbf{n}})\hat{P}(\mathbf{n},t)$$

at equilibrium $\hat{P}_0(\mathbf{n}) = \exp[\beta(\Omega_0 + \sum_{\alpha} \mu_{\alpha} \sum_i n_i^{\alpha} - \hat{H})]$

with $\hat{H} = \frac{1}{2!}\sum_{\alpha,\beta,i\neq j} V_{ij}^{\alpha\beta} n_i^{\alpha} n_j^{\beta} + \frac{1}{3!}\sum_{\alpha,\beta,\gamma,i\neq j\neq k} V_{ijk}^{\alpha\beta\gamma} n_i^{\alpha} n_j^{\beta} n_k^{\gamma} + \ldots$

- Under imposed chemical potential gradient:
  introduce effective interactions so as to satisfy steady state

$$\hat{P}(\mathbf{n},t) = \hat{P}_0(\mathbf{n})\hat{P}_1(\mathbf{n},t); \quad \hat{h}(t) = \frac{1}{2!}\sum_{\alpha,\beta,i\neq j} \upsilon_{ij}^{\alpha\beta}(t) n_i^{\alpha} n_j^{\beta} + \frac{1}{3!}\sum_{\alpha,\beta,\gamma,i\neq j\neq k} \upsilon_{ijk}^{\alpha\beta\gamma}(t) n_i^{\alpha} n_j^{\beta} n_k^{\gamma} + \cdots$$

$$\frac{d\langle n_i^{\alpha}\rangle}{dt} = -\sum_{s\neq i} J_{i\to s}^{\alpha} \text{ and } \frac{d\langle n_i^{\alpha} n_j^{\beta}\rangle}{dt} = 0$$

➔ Linear system relating effective interactions and gradient of μ's

Kinetic Coupling: Self-Consistent Mean-Field Model (2)

- The effective interactions contain the kinetic coupling terms

$$J_{i\to j}^{\alpha} = -L_{ij}^{(0)\alpha}\left(\delta\mu_j^{\alpha} - \delta\mu_i^{\alpha}\right) + \sum_{\sigma,s} L_{ijs}^{(1)\alpha\sigma}\left(\upsilon_{js}^{\alpha\sigma} - \upsilon_{is}^{\alpha\sigma}\right) + \ldots$$

becomes $\boxed{J_{i\to j}^{\alpha} = -\sum_{\beta,s,s'} L_{ij,ss'}^{\alpha\beta}\left(\mu_{s'}^{\beta} - \mu_s^{\beta}\right)}$ ➔ full Onsager Matrix

- Approach can be extended to arbitrary crystallographic structures
- Requires knowledge of atomic jump frequencies

➔ Allows for including stress effects on kinetics:

e.g., **creep, transport near dislocations**

Anisotropy in solute drag due to tetragonal strain

Tetragonal strain with δ= ± 0.01

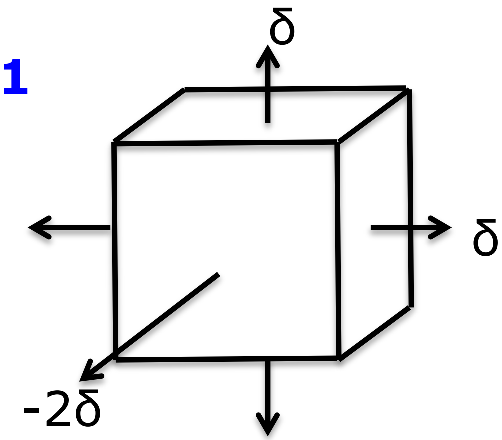

- L_{SiSi} > 0 in the entire temperature range
- L_{SiV} is *positive* if solute-drag is predominant

Perpendicular to the elongation axis

Parallel to the elongation axis

Strain free T_s ≈ 950 K

δ = - 0.005

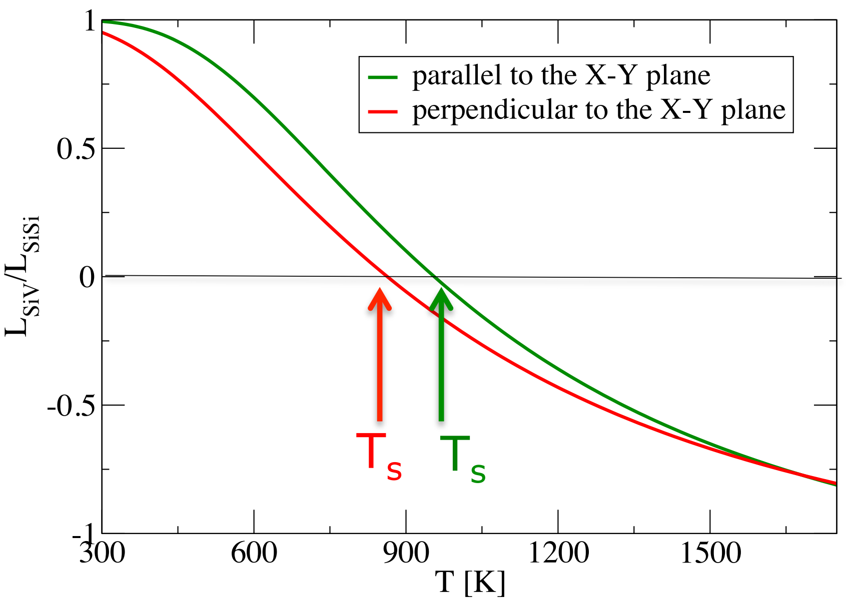

δ = 0.005

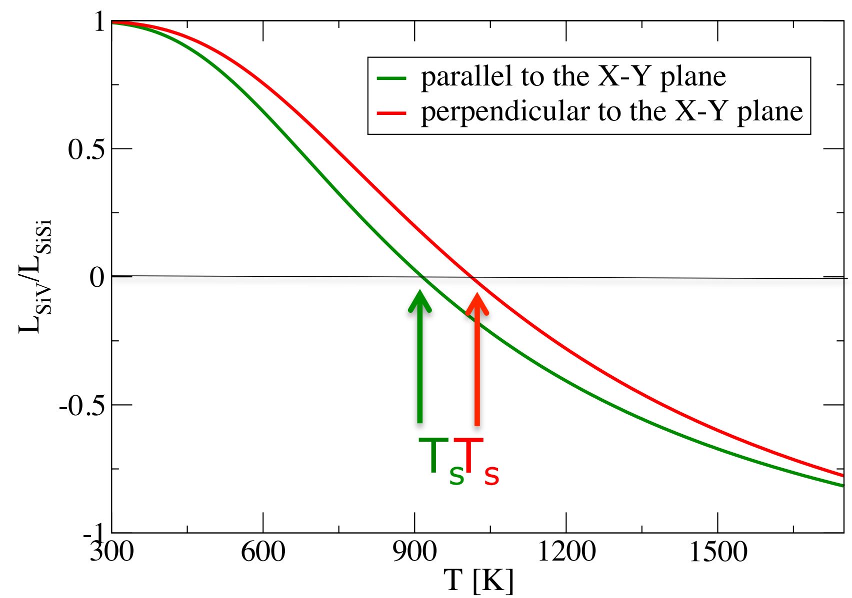

Anisotropy in solute drag due to tetragonal strain

- $L_{SiSi} > 0$ in the entire temperature range
- L_{SiV} is *positive* if solute-drag is predominant

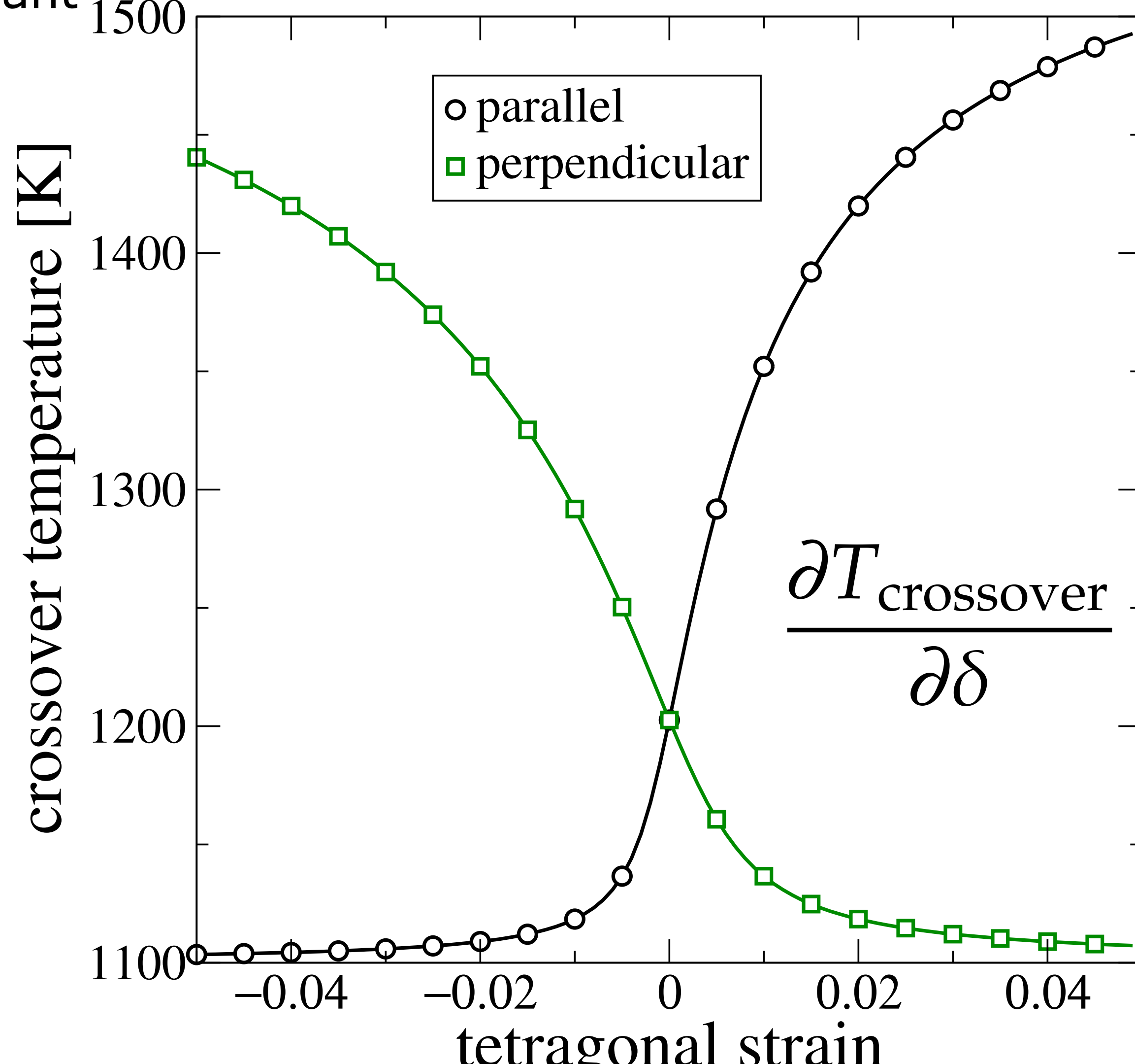

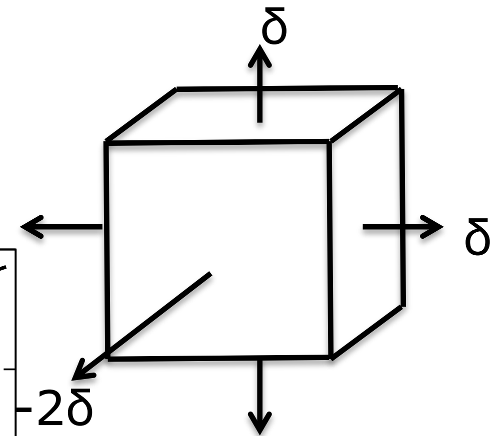

$$\frac{\partial T_{\mathrm{crossover}}}{\partial \delta} = 1.92 \times 10^4\ \mathrm{K}$$

Dislocation strain field

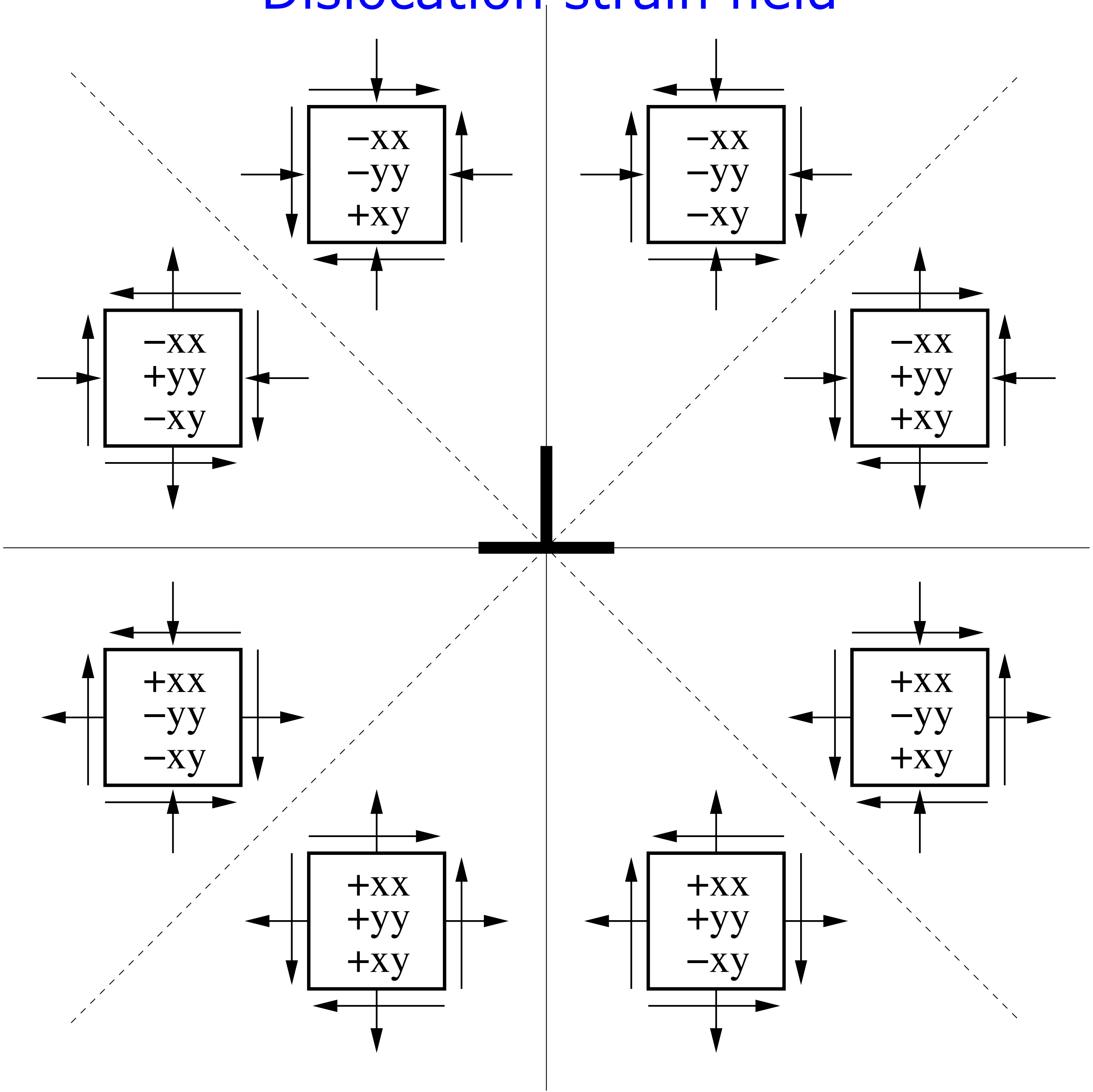

Dislocation strain field

$$\varepsilon_{\mathrm{volumetric}} = -\frac{b}{4\pi r}\sin\theta$$

$$\gamma_{\mathrm{shear}} = \frac{b}{4\pi r}\frac{3}{2}\cos\theta\cos 2\theta$$

$$\varepsilon_{\mathrm{bb}} = -\frac{b}{4\pi r}\left(2\sin\theta + \frac{3}{2}\sin\theta\cos 2\theta\right)$$

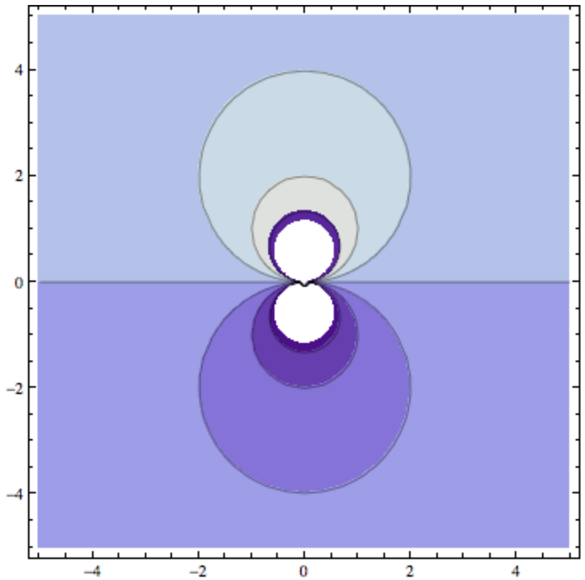

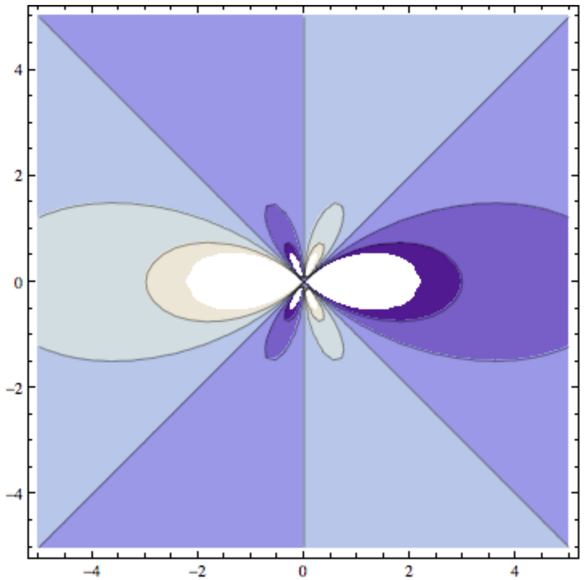

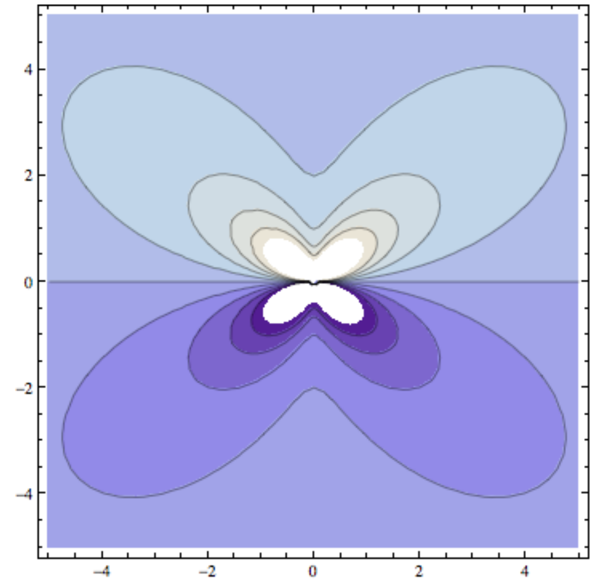

Anisotropy in L_{SiV} due to dislocation strain field

$$\varepsilon_{\text{volumetric}} = -\frac{b}{4\pi r}\sin\theta$$

$$\gamma_{\text{shear}} = \frac{b}{4\pi r}\frac{3}{2}\cos\theta\cos 2\theta$$

$$\varepsilon_{\text{bb}} = -\frac{b}{4\pi r}\left(2\sin\theta + \frac{3}{2}\sin\theta\cos 2\theta\right)$$

$$\begin{pmatrix} L_0 + \frac{1}{3}L'_{\text{v}}\varepsilon_{\text{volumetric}} + \frac{1}{6}L'_{\text{tet}}\varepsilon_{\text{bb}} & -\frac{2}{3}L'_{\text{tet}}\gamma_{\text{shear}} \\ -\frac{2}{3}L'_{\text{tet}}\gamma_{\text{shear}} & L_0 + \frac{1}{3}L'_{\text{v}}\varepsilon_{\text{volumetric}} \end{pmatrix}$$

L0: unstrained L
L'_v: volumetric strain derivative
L'_{tet}: tetragonal strain derivative

Anisotropy in L_{SiV} due to dislocation strain field

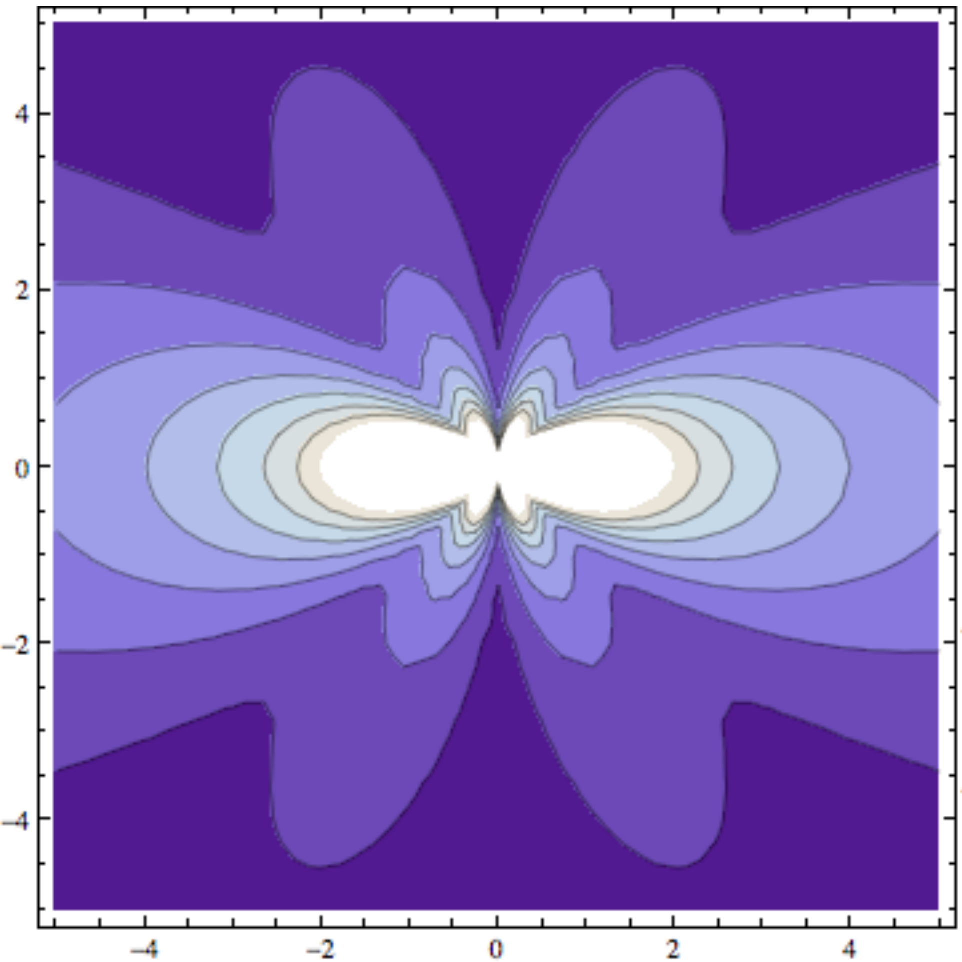

difference between max. and min. eigenvalue of Lij

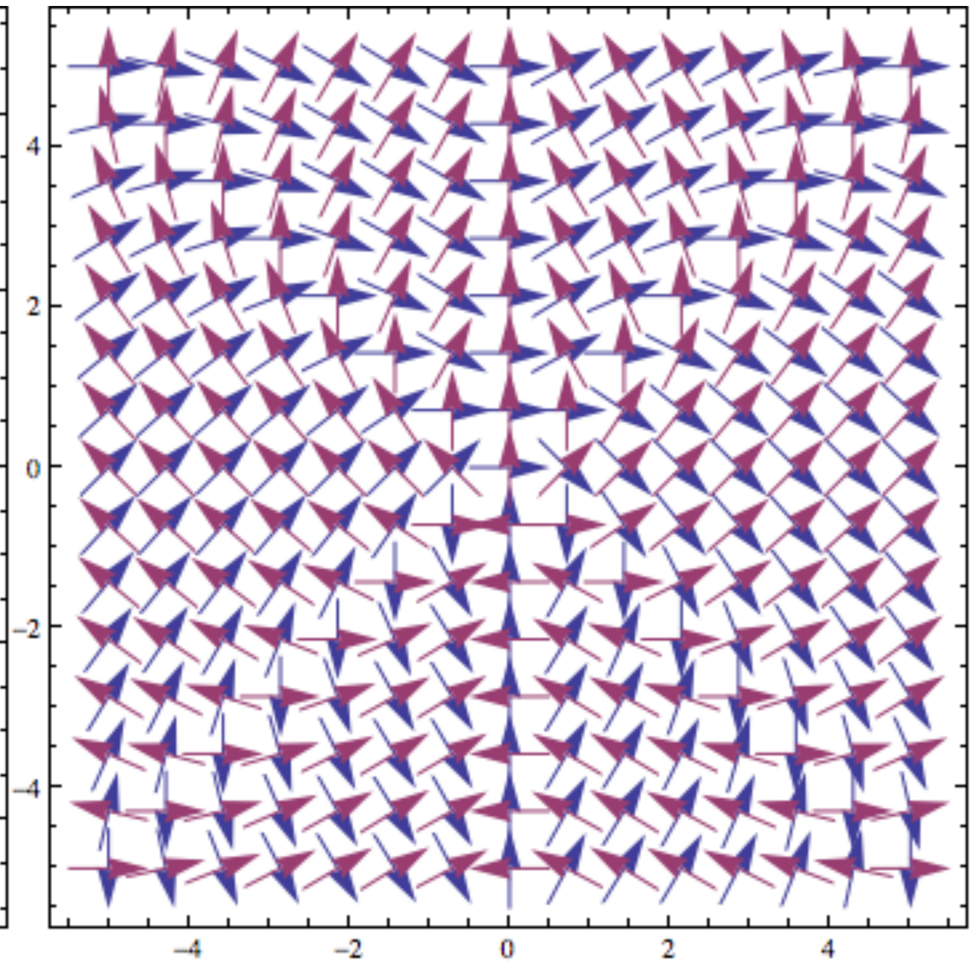

orientation of max. and min. eigenvectors of Lij

Anisotropy in L_{SiV} relative to average L_{SiV} at crossover

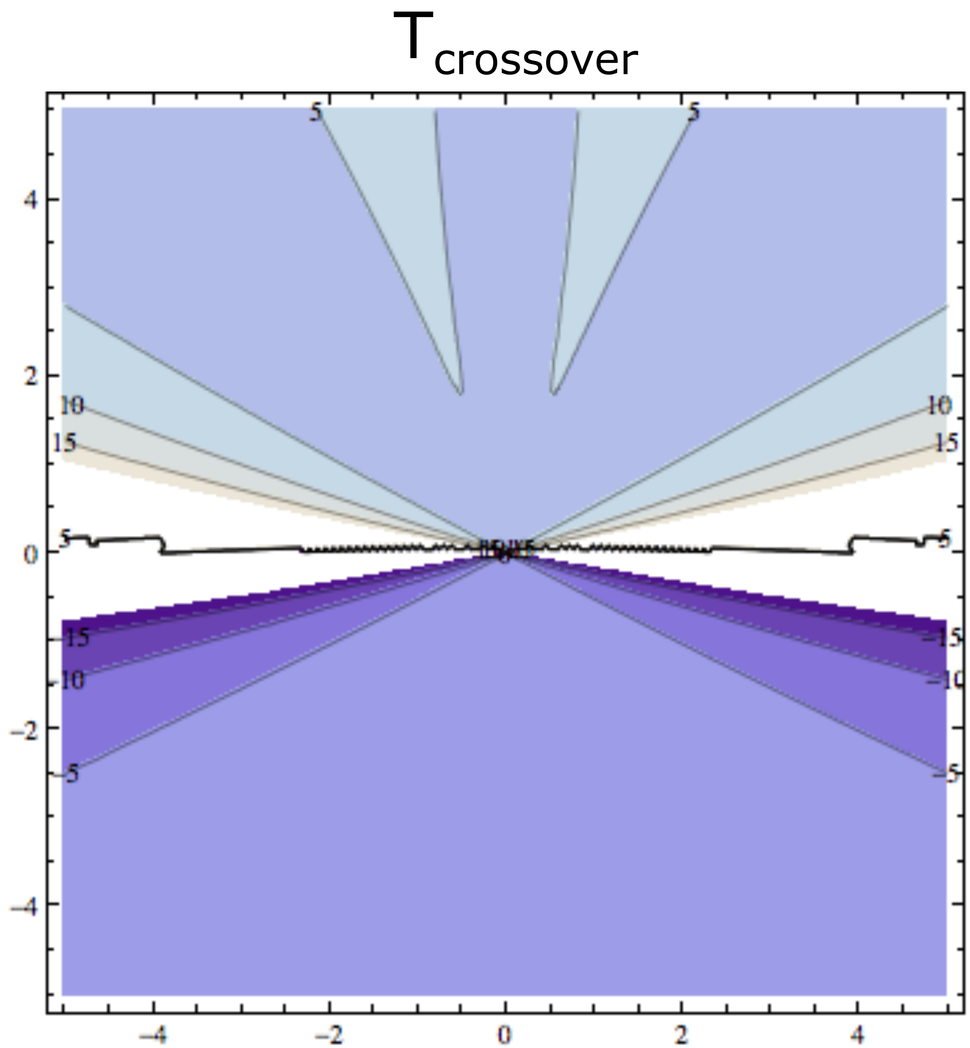

unstrained L nearly 0: ratio nearly distance independent

Anisotropy in L_{SiV} relative to average L_{SiV} below crossover

$T_{crossover} - 100K$

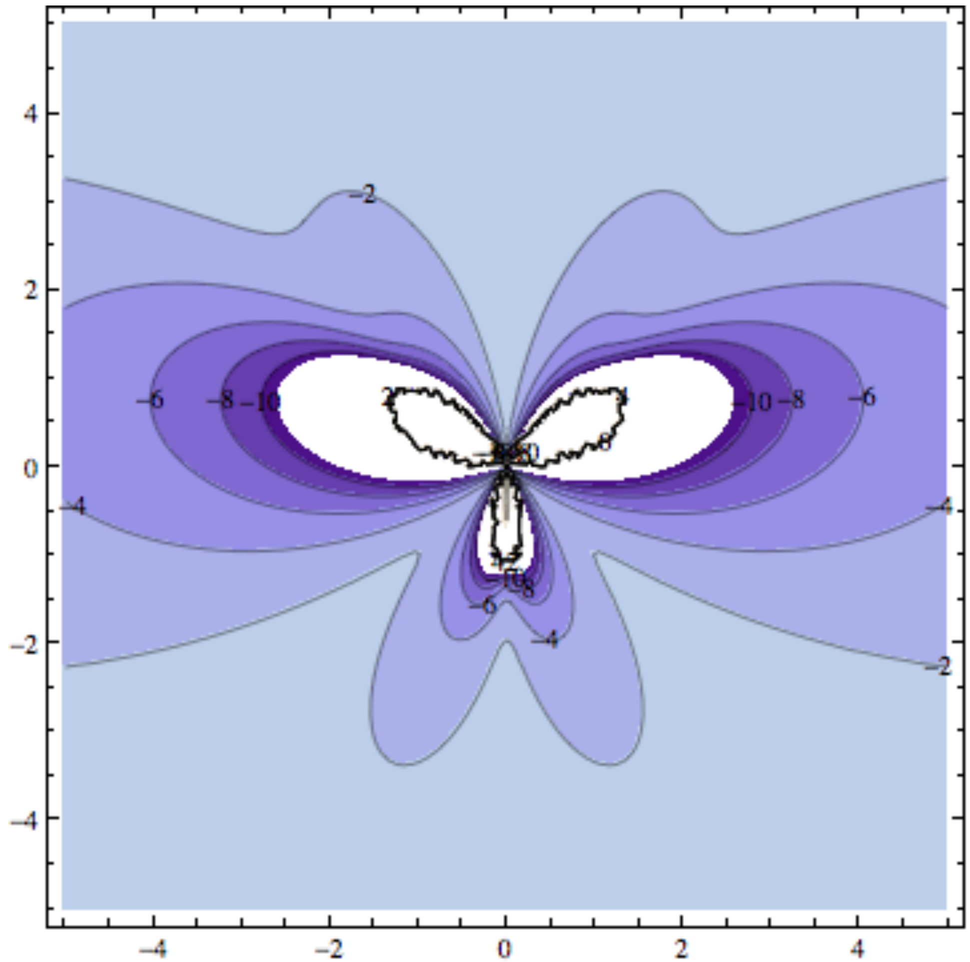

extremely large anisotropies near core
unusual contours should affect solute distribution

Anisotropy in L_{SiV} relative to average L_{SiV} above crossover

$T_{crossover}$+100K

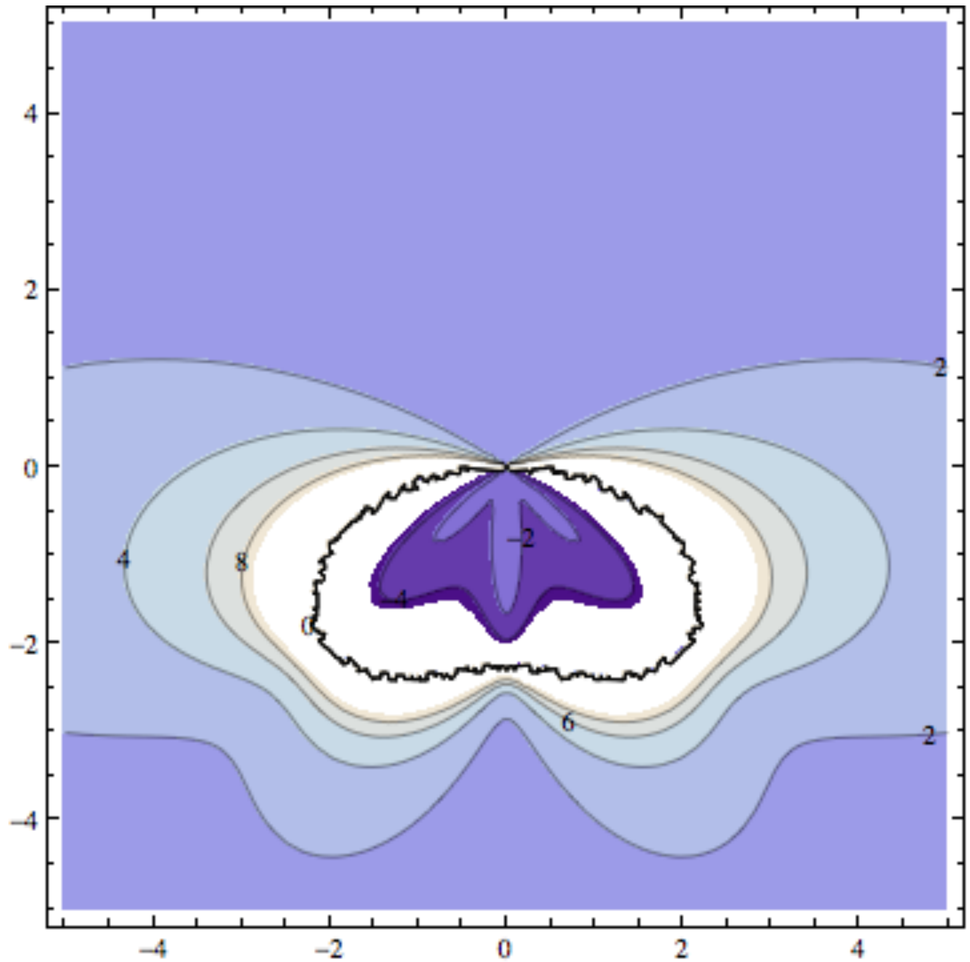

extremely large anisotropies near core
unusual contours should affect solute distribution

Initial flow streams at $T_{crossover}$

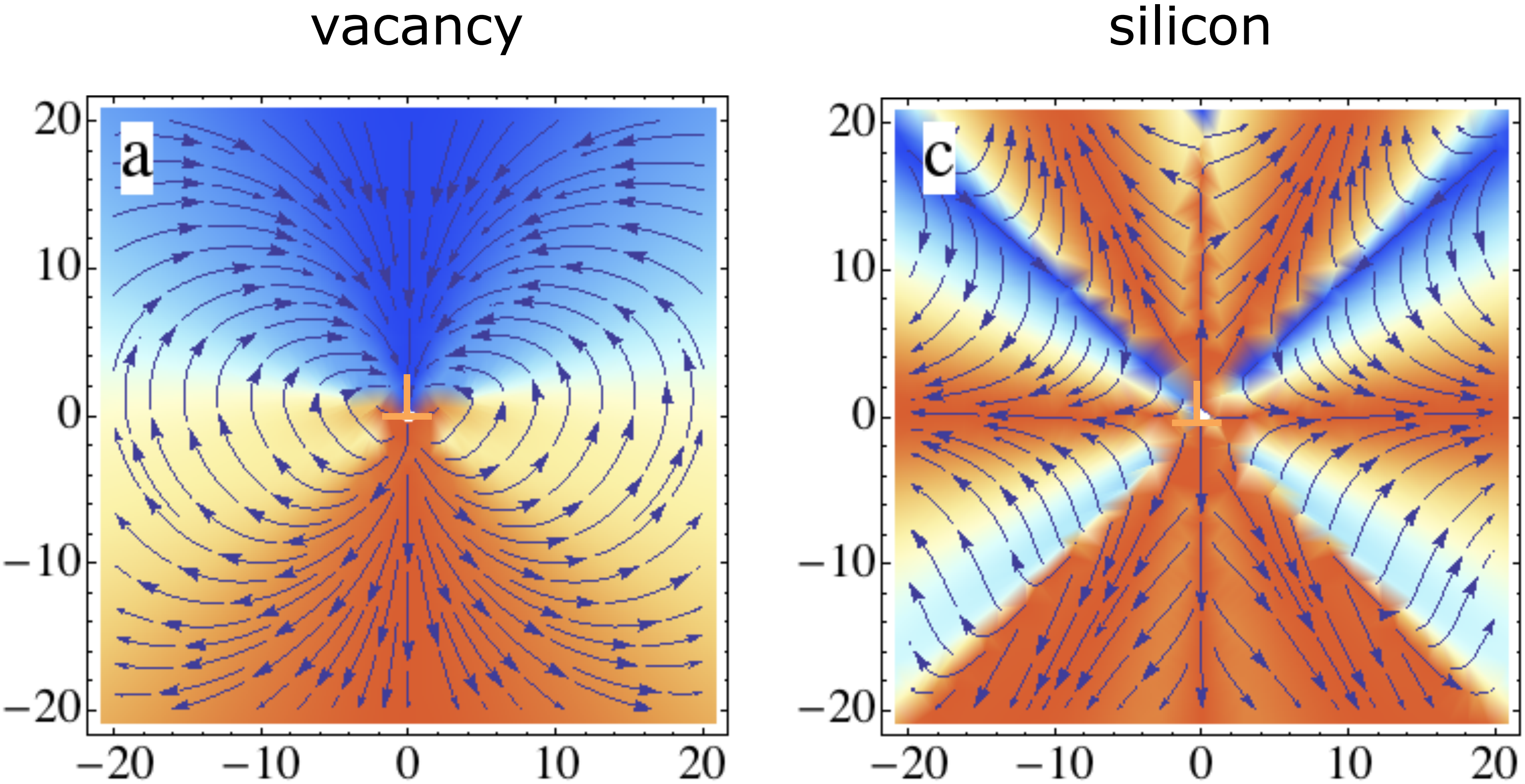

strong directionality from primary anisotropy at crossover

Initial flow streams at $T_{crossover} - 50K$

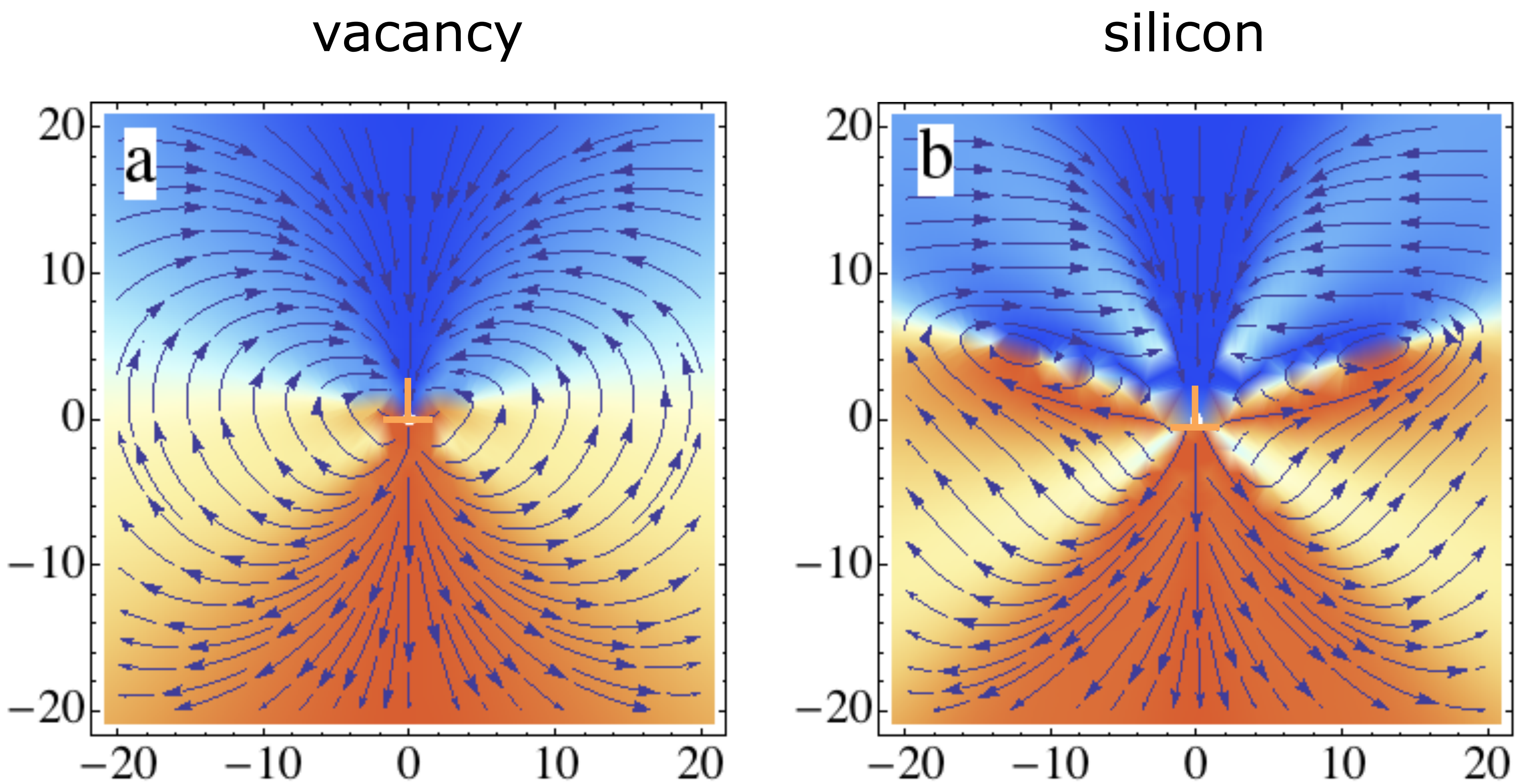

solute drag into core in anisotropic pattern

Initial flow streams at $T_{crossover}$+50K

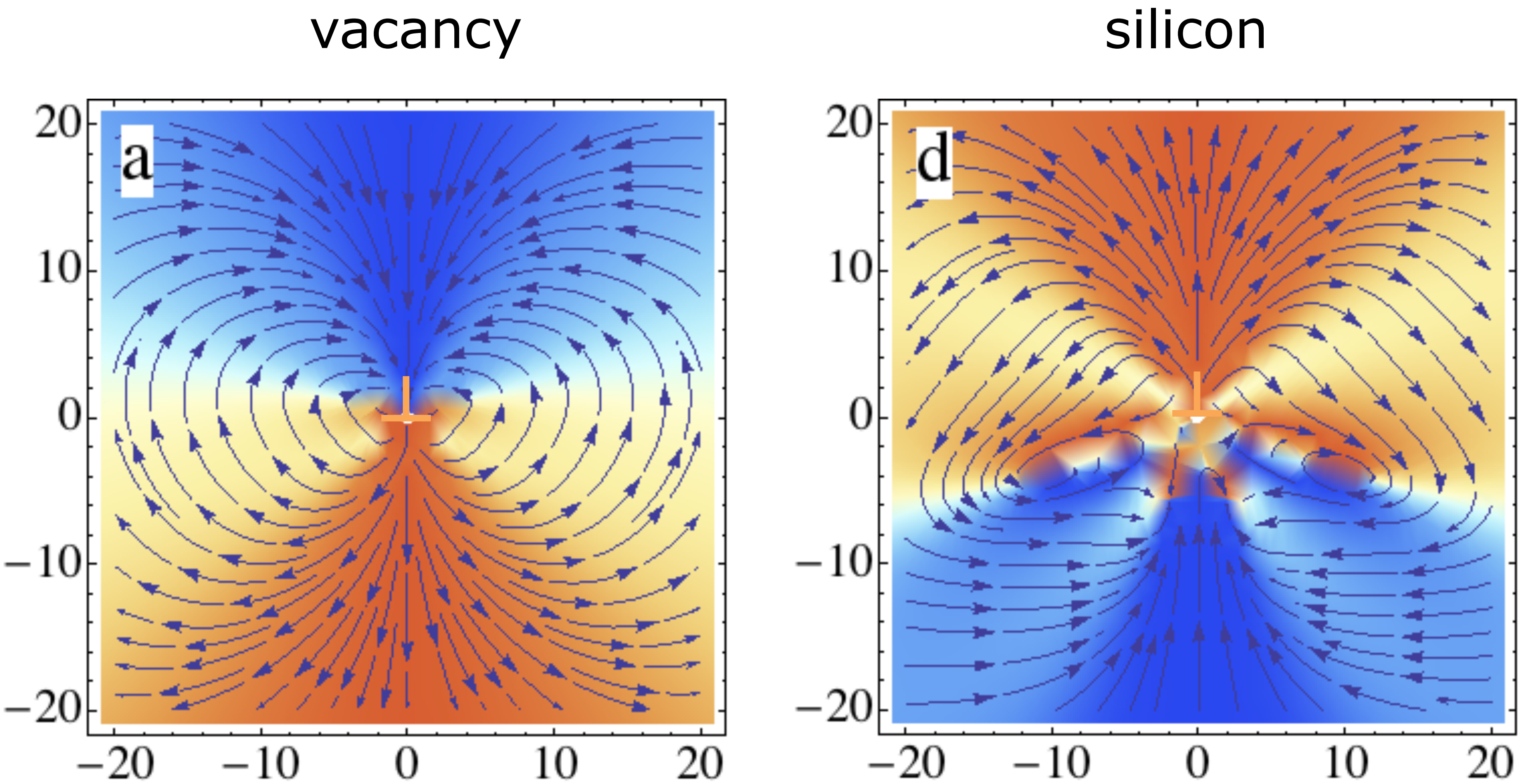

depletion of solute from dislocation core above crossover (solute exchange)

Stress-induced anisotropic diffusion in alloys: Complex Si solute flow near a dislocation core in Ni

Venkat Manga, Zebo Li, *Thomas Garnier*, *Maylise Nastar*, Pascal Bellon, Robert Averback, **Dallas R. Trinkle**

Materials Science and Engineering, Univ. Illinois, Urbana-Champaign

CEA Saclay, Service de Recherches de Métallurgie Physique, France

Goal: Predict solute and defect evolution near a dislocation

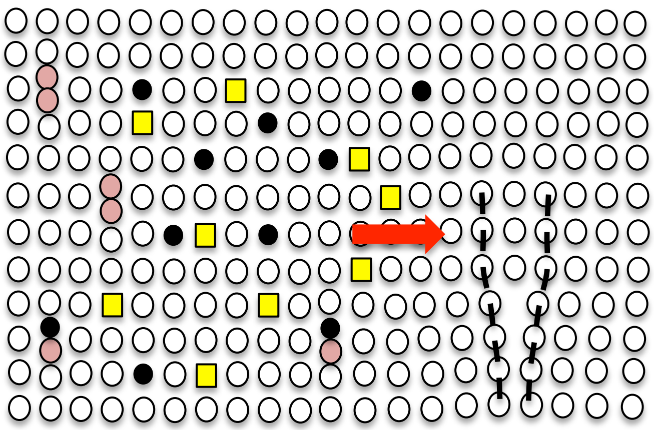

Transport of point defects near dislocations (sinks)

Under irradiation: continuous transport of defect fluxes to sinks

- Coupling of defects and solutes fluxes?
- Segregation, precipitation, creep?

Stresses of dislocation and applied

- Inhomogeneous driving forces
- Inhomogeneous anisotropic mobilities

System: substitutional Si in Ni

Approach:

- Ab initio calculation of migration barriers
- Self-consistent mean-field method

U.S. DEPARTMENT OF ENERGY | Office of Science

BES DE-FG02-05ER46217 & NERSC